Spatial-temporal Assessment of historical and projected drought events over Isiolo County, Kenya using Self Calibrating Palmer Drought Severity Index

phillip Ochieng (koderaphillips@yahoo.com)
University of Nairobi https://orcid.org/0000-0002-9989-4141
Isaiah Nyandega
University of Nairobi
Boniface Wambua
University of Nairobi

Research Article

Keywords: scPDSI, CHIRPS, scPDSI, CORDEX, EOF

Posted Date: February 11th, 2021

DOI: https://doi.org/10.21203/rs.3.rs-220061/v1

Spatial-temporal Assessment of historical and projected drought events over Isiolo County, Kenya using Self Calibrating Palmer Drought Severity Index

Phillip Ochieng[1,2*], Isaiah Nyandega[21] Boniface Wambua[31]

[1]Department of Geography and Environmental Studies, University of Nairobi

P.O. Box 30197-00100 GPO, Nairobi, Kenya

[2]Kenya Meteorological Services, P.O. Box 30259-00100 GPO, Nairobi, Kenya

Corresponding Author: Phillip Ochieng [1,2*] E-mail:koderaphillips@yahoo.com

Abstract

This study was to determine the spatiotemporal characteristics of historical and projected drought events throughout Isiolo County, Kenya, through using self-calibrating Palmer drought severity index (scPDSI). The scPDSI is a complex and robust drought index that applies the water balance model by incorporating the role played by evapotranspiration and soil properties on drought analysis therefore making it appropriate to identify the linkages between meteorological, agricultural and hydrological droughts. The historical scPDSI was computed at a monthly timescale using a 39-year long monthly mean precipitation data from Climate Hazard Group Infrared Precipitation with Station (CHIRPS) and monthly average temperature data from the Climate Research Unit (CRU). The climatological (1950-1996) available water holding capacity (AWHC) of the soil was obtained from Oak Ridge National Laboratory Distributed Active Archive Center (ORNL DAAC) for biochemical dynamics at a spatial resolution of 1^o x 1^o. The projected scPDSI under Representative Concentration Pathways (RCPs) was computed using bias corrected monthly temperature and precipitation model output data from Coordinated Regional Climate Downscaling Experiment (CORDEX). The datasets were extracted for ten grid points in the County. The scPDSI was used to assess the historical and projected duration, severity, and intensity of droughts. The major significant historical and projected drought events and their characteristics were clearly identified using the run theory. ScPDSI runs have shown that more severe drought events dominated the period between 1980 and 2000. ScPDSI had the longest dry event duration of 61 months and a severity of 126.412 with adverse effects on the eastern locations. The projected drought events identified Mar 2046 –Mar 2048 under RCP4.5 to

be the most severe drought lasting for 25 months with severity of 59.292 while under RCP8.5 run Nov 2042 – Nov 2046 is identified as the most severe, 114.362 with the duration of water stress anticipated to last for 49 months.

To examine the spatial variability of the drought events in the County, the Empirical Orthogonal Analysis (EOF) was applied to the historical and projected scPDSI time series. The EOF results indicated that the two leading eigen vectors accounted for over 85% of the spatial variability for both historical and projected droughts under the RCPs. Subsequently, the Mann-Kendall (MK) test was applied to the projected scPDSI, temperature and precipitation timeseries in order to determine the local expected drought trends. The MK test of the identified significant increase in trend for temperatures under RCP8.5 and precipitation under RCP4.5 towards the end of the last decade under the study period considered. Both scenarios showed a decline in trends of drought events in Isiolo County from 2020-2050.

1 INTRODUCTION

Drought is a natural meteorological phenomenon with widespread impacts that cut across many socio-economic sectors of any society with devastating effects on community (Dai, 2013a; Mishra & Singh, 2010, 2011; Polong et al., 2019). The effects of drought are anticipated to be amplified in terms of complexity, frequencies, and extent as consequence of climate change and variability (Dai, 2011; Sheffield et al., 2012). An exhaustive drought analysis is fundamental for drought management and alleviation and subsequently can improve drought forecasting (Zargar et al., 2004) .

Drought indices are commonly applied methods to describe and quantify drought conditions. The indices use climatic variables such as precipitation, air temperature, evapotranspiration, soil moisture, and stream-flow to quantitatively measure drought characteristics (Abdulrazzaq et al., 2019; Hao & AghaKouchak, 2013). Over 150 indices have since been established based on the above indicators (Kalisa et al., 2020; Patil, 2020). Numerous drought indices have effectively been applied as drought analysis tools worldwide (Barua et al., 2010; Dai, 2011). Indices are invented or modified for various geographical locations, purposes, and demands (Zargar et al., 2004). Currently, the major drought indices include Palmer Drought Severity Index based on temperature and rainfall (Aiguo et al., 2004; Palmer, 1965; Trenberth et al., 2014), the Standard Precipitation Index based on rainfall only (Ayugi et al., 2020a; Mckee et al., 1993; Wambua et al., 2018) and the standardized precipitation evapotranspiration index based on evapotranspiration and temperature (Dei, 2009; Polong et al., 2019; Tirivarombo et al., 2018). Since the use of drought indices tends to vary by specific place and function, there is a need to establish the most accurate drought indices for geographical location and application so that the quantification and classification of drought can be accurate (Ayugi et al., 2020b; Dai, 2013b; Zargar et al., 2004).

The Palmer Drought Severity Index (PDSI) introduced by Wayne Palmer in 1965 is commonly believed to have laid the foundation for drought forecasting and analysis. The PDSI (Palmer, 1965) is among the frequently used drought monitoring tools in the United States and worldwide (Dai, 2011; Enfoque et al., 2010; Mishra & Singh, 2011). PDSI is widely being used to predict the onset and the cessation of an anticipated drought event. The PDSI has extensively also been

discussed in-depth by (Wells et al.,, 2004; Alley, 1984; Dai, 2011). Unlike other previously mentioned Drought Severity Indices, using temperature and soil properties in the PDSI computation and precipitation data is the core strength. Moreover, it is scientifically possible that while rainfall stress is the main predictor of drought, the temperature has a central role in triggering drought (Chen & Sun, 2015; Shi et al., 2017). Additional weather variables integrated into calculation make PDSI suitable to connect meteorological drought, hydrological and agricultural drought (Wanders et al., 2010). Previous studies suggest that PDSI does not capture well drought in locations with extreme variability in rainfall or runoff, for example, in Australia and Southern Africa (Hayes et al., 1999). These limitations identified by Alley in 1984 and have since been addressed by modification of the original model into a self-calibrating version (Wells et al., 2004; Liu et al., 2017). The original PDSI lacks the ability to geographically compare drought which leads to poor representation of drought in other locations other than the few locations sampled by Palmer. The detailed modification of the original PDSI to a self-calibrating PDSI is explained in detail by (Wells et al., 2004) as discussed in methodology section in this paper.

************Table 1************

The objective of this study is to determine the spatial-temporal variability of historical and projected drought characteristics in Isiolo County, Kenya based on the assessment of the severity of dry events in the County. The study precisely focused on (1) Determine the spatial and temporal evolution of historical droughts based on Empirical Orthogonal Function analysis and use the results to validate the performance of scPDSI based of observed historical droughts (2) Compute projected scPDSI based on RCP4.5 and RCP8.5 from CORDEX model outputs (3) Determine the historical and projected drought trends over Isiolo County based on sequential Mann-Kendall trends analysis. The findings of this study are intended to improve the science of drought prediction and knowledge of drought and its characteristics in Isiolo County. This will complement the efforts of local and national government in planning for long term drought resilience actions and prepare for contingency response actions.

2 Data and methodologies

2.1 Study area

Isiolo County has two sub-counties namely (Isiolo North and Isiolo South). Owing to the expansive nature of the two sub-counties drought response is always untimely. Isiolo County is located in Kenya and lies between Longitudes 36.8333^{o} East and 39.8333^{o}'East and latitude 0.0833^{o}South and 2^{o} North. It covers an area of approximately 25,700 km^{2}. Isiolo town lies 285 kilometers north of Nairobi, capital city of Kenya, if accessed through the great north road.

***********Figure 1**********

In general, Isiolo County just like the rest of the country, experiences bi-modal rainfall pattern influenced by the North-South movement of the Inter-Tropical Convergence Zone (ITCZ) with long rains received from March to May and short rains received from October to December with peaks observed in April and November. The maximum temperature generally rises from November with the highest temperatures experienced during the months of February. Isiolo County is characterized by three climatic zones namely; semi-arid, arid and very arid. The characteristics of these climate zones are as follows: Semi-arid zone IV (Central and Kinna divisions. The annual rainfall received in these locations range from 250-650mm. Arid Zone V - Central Garbatulla division with an annual rainfall of between 300-350 mm and can only support annual grasslands and a few shrubs. Very Arid Zone VI which is mostly in Meriti and Sericho divisions which covers the largest percentage of the land area of the county. The rainfall received here is between 150 and 250mm per year.

***********Figure 2************

*****************Figure 3************

2.2 Data

This study applied the monthly gridded of temperature dataset for the computation and modification of the projected Thornthwaite Evapotranspiration at spatial resolution of 0.5 ^{o} x 0.5 ^{o} from Climate Research Unit, CRUTS4.03 (Harris et al., 2014). CRU temperature dataset successfully applied by (Polong et al., 2019) in the computation of potential evapotranspiration over Tana River basin, Kenya. Monthly precipitation datasets obtained from Climate Hazard Group Infrared Precipitation with Station (CHIRPS v2; Funk et al.,2015). The CHRPS data product has a spatial resolution of 0.05 (~5.3 km). The historical scPDSI was also obtained from

CRU version 4.04 of high-resolution gridded data at 0.5 ^{o} x 0.5 ^{o}. This data was used to validate the self-computed scPDSI. All the aforementioned datasets are analyzed at a temporal resolution of 1980-2018.

The representative concentration pathway data outputs are available on Coordinated Regional Climate Downscaling Experiment (CORDEX) Africa domain and have a spatial resolution at grid increment of 0.25° × 0.25° (~25 km × 25 km) and at a temporal scale of 1951 to 2005 for historical runs and future projections from 2006 to 2100. This dataset has widely been used in the study of the future scenarios of temperature, rainfall and drought characterization (Tan et al., 2020; Ayugi et al., 2020b; Ongoma et al., 2018) over East Africa region. The results depicted a better representation of rainfall and surface temperature trends. The models were further bias corrected using quartile mapping approach in order to reduce errors in projected drought scenarios.

The climatological Soil Available Water Holding Capacity (AWHC), also referred as AWC or Root Zone Water Holding capacity was obtained from Oak Ridge National Laboratory Distributed Active Archive Center (ORNL DAAC) for biochemical dynamics at a spatial resolution of 1^{o} x 1^{o} (https://daac.ornl.gov/cgi-bin/dsviewer.pl?ds_id=548). This dataset has extensively been applied by (Rosenzweig & Ridge, 1986; Liu et al., 2017) in computing scPDSI. All the gridded datasets applied in this study was extracted and analyzed from the 10 grid points as shown in figure 1.

2.3 Methodologies

2.3.1 Computation of Self-Calibrating Palmer Drought Severity Index (sc-PDSI)

The procedure of calculating Palmer Drought Severity Index relies upon the principle that the evapotranspiration (ET), recharge (R), runoff (RO), loss (L), potential evapotranspiration (PE), potential recharge (PR), potential runoff (PRO), and potential loss (PL) are derived from the meteorological and soil data. The PE is estimated using (Thornthwaite, 1948) approach and majorly depend on the AWHC of the soil.

The water balance equation was set up based on (Wells et al., 2004). This formed the foundation for the computation of the moisture anomaly; which is the difference between actual precipitation and potential precipitation. A detailed step by step calculation of PDSI and modification to scPDSI can be found in (Wells et al., 2004) and is summarized as; First the

moisture departure and moisture anomalies based on water balance model is computed. The rationale of the climate characteristic, K, is to modify the theoretical value of D based to the characteristics of the climate in a manner that PDSI values over spatiotemporal scale can be accurately compared.

$$K_i' = 1.5\mathrm{Log}_{10}\left[\frac{\frac{\overline{PE}_i+\overline{R}_i+\overline{RO}_i+2.8}{\overline{P}_i+\overline{L}_i}}{\overline{D}_i}\right] \quad (1)$$

$$\tilde{Z} = \sum_{j=1}^{12}\left|\overline{d}_j\right|K_j' \quad (2)$$

$\tilde{Z}$ is regarded as the summation of average annual moisture departure and D_i is the mean moisture anomaly for the a specic month. The duration factors are then computed based on K_i'. In particular, the certain predefined PDSI value X_i is a weighted sum of the previous PDSI value X_{i-1}, which denotes the current climate trend, and the current moisture anomaly Z_i, which is how wet or dry it has been over the current period.

$$X_i = pX_{i-1} + qZ_{i*} \quad (3)$$

In real terms, the duration factors explain the sensitivity of the index is to precipitation changes and the deficit thereof, p= 5 0.897 and q = 1/3. Sequentially the 98th and 2d percentile values of the PDSI then finally SC-PDSI is computed as.

$$X_t = \left(1 - \frac{m}{m+b}\right)X_{i-1} + \frac{CZ_t}{m+b} \quad (4)$$

Thus, considering any category of drought, specified as C, the computed index is calibrated as long as m and b can be computed, where m is the line slope and b is the y intercept.

2.3.2 Identification of Drought Signals Using Empirical Orthogonal Function Analysis

EOF analysis is one of the most popular statistical methods used to identify signals in spatial data. It's used to get rid of noise inherent in most climate data (Lorenz, 1956; Polong et al., 2019). The method involves mapping the data onto a new frame which creates variability in the original data. Thus, the process ideally produces modes (or eigenvectors) which are equal in

number to the original data. The modes are orthogonal to each other meaning that each of them is uncorrelated with the others. Ideally, the first few modes contain the biggest percentage of the variability in the original data while the rest explain minimal variability and can be regarded as noise. EOF can be mathematically expressed as;

$$\begin{Bmatrix} Y_{i,1} = a_{11}X_{i,1} + a_{12}X_{i,2} + \cdots + a_{1k}X_{i,k} \\ Y_{i,2} = a_{21}X_{i,1} + a_{22}X_{i,2} + \cdots + a_{2k}X_{i,k} \\ \vdots \\ Y_{1,k} = a_{k1}X_{i,k} + a_{k2}X_{i,2} + \cdots + a_{kk}X_{i,k} \end{Bmatrix} \quad (5)$$

The original correlated scPDSI values at different grid points are $X_{i,1}X_{i,2} \ldots\ldots, X_{i,k}$ where k refers to the number of the grid points chosen for this study in the Isiolo County (=10) and i denotes the length of scPDSI series at each grid point. The eigen values $Y_{i,1}, Y_{i,2}, \ldots\ldots, Y_{i,k}$ are simultaneously produced.

2.3.3 Mann-Kendall Trend Analysis

Mann-Kendall (MK) test statistics was applied to depict future trends of drought, temperature and rainfall in Isiolo County. MK test statistics is a nonparametric trend test technique. This method commonly used in the science of hydrology and climatology for testing randomness of the temporal variation in hydro-meteorological data series. It is widely applied in detecting the significant changes in trends of a time series (Yilmaz, 2019; Xing etal., 2018). MK is a rank-based technique, it is not influence by the extremes and therefore best suited for skewed data i.e., it is not affected by the outliers like the simple linear regression method.

MK test statistics

$$S = \sum_{i=2}^{n} \sum_{j=1}^{i=1} sign(x_i - x_j) \quad (6)$$

Where the x_j are the sequential data values, n is the length of the time-series, and sign $sign(x_i - x_j)$ is −1 for $(x_i - x_j) < 0; 0\ for\ (x_i - x_j) = 0, and\ 1\ for\ (x_i - x_j) > 0$. MK test was used to recognize patterns that are statistically significant at the 95% confidence level. In this approach, the null hypothesis H_o was that there is no a trend in projected drought, temperature and rainfall in Isiolo County; alternative hypothesis H_a was that there is increasing and/or decreasing trends.

Sneyers (1990) presented sequential values, $u(t)$ and $u'(t)$, from the Mann-Kendall test's progressive testing to identify the abrupt change of trend with time. Here, $u(t)$ is a standardized variable with a unit standard deviation and zero mean. Its sequential pattern therefore fluctuates around the level of zero. As follows, the sequential Mann-Kendall can be summarized stepwise,

1. The values of x_j annual mean time series are compared with the x_i where (($j = 1,2, \dots \dots, n$ and $i = 1, \dots \dots, j-1$) at each comparison the instances where $x_j > x_i$ are noted by n_j.
2. The statistics t is computed using

$$t_j = \sum_1^j n_j \tag{7}$$

3. The mean and the variance are then computed using

$$E(t) = \frac{n(n-1)}{4} \tag{8}$$

$$Var(t_j) = [\frac{j(j-1)(2j+5]}{72} \tag{9}$$

4. The sequential values of the statistic $u(t)$ are then calculated as

$$u(t) = \frac{t_j - E(t)}{\sqrt{Var(t_j)}} \tag{10}$$

The values of $u'(t)$ are simultaneously calculated in a reverse sequence from the end of the time series.

2.3.4 Characterization of Drought Using Runs Theory

A run is a sequence of one or more observations of different kinds preceded and succeeded by the same type of observations. The run method is founded on a threshold level selection, Q (Le et al., 2019; Yevjevich, 1969). Thus, any drought event can be described by: duration, Du, the number of consecutive intervals of time (T) under which the rainfall appears below critical threshold; cumulative deficiency, the total amount of successive deficits; and; intensity, I(s) by the ratio of severity and duration of the drought event. It is possible to fully comprehend the concept as below.

***********Figure 4***********

Frequency, F of the dry events considered in this study were scPDSI ≤ -1 category over a period of time N (months) are the chances of occurring drought, calculated as the ratio of total drought duration and the total time N: The drought frequencey, F, can therefore be described as

$$F_j = \frac{\sum_{i=1}^{m} Du_i}{N} \times 100\% \quad (11)$$

N is the drought periodic time and *m* is the number of drought events in a given Palmer category/class; consequently, the degree of severity, S, a drought event can be computed using

$$S_j = \sum_{k=1}^{D_u} scPDSI_k \,|scPDSI_k < Q_j \quad (12)$$

Q refers to the set drought index threshold as described earlier.

3 Results and Discussions

3.1 Spatial-Temporal Characteristics of Historical Dry Events in Isiolo County

The temporal series of scPDSI calculated over 39 years between 1980 and 2018 were analyzed for spatial signals to determine the geographical extent of mild-severe drought events over Isiolo based on simple covariance matrix EOF analysis. The results presented in figure 5 indicates that the two leading EOFs accounted for a total 100% of spatial variability.

******************Figure 5********************

The first EOF loading is univariant with spatially homogeneous positive values. The second EOF loading depicted both negative and positive variability over Isiolo County. These results show that both dry and wet events would have been experienced over Isiolo County over the review period. The second EOF loading characterizes more localized events (Santos et al. 2010; Polong et al., 2019), this is also coherent with figure 2. The southern and western sectors of the County are not as adversely affected by drought to high annual rainfall amounts and low temperatures as a result of geographical proximity to Mount Kenya as compared to Eastern sectors that generally receives suppressed rainfall amounts and high temperatures.

The temporal interannual evolution two corresponding EOF scPDSI time series (figure 6) shows that a total of 15 dry events and 12 wet events were experienced in Isiolo County. The period in

which the dry events were experience during study period is shown in table 2. These results are in concurrence with Balint et al., 2011 and Mwangi et al., 2013 studies which identified 1983-1984, 1992-1993, 1999-2000, and 2009-2011 as some of the drought years though using different approaches to study drought.

**********Figure 6**********

The characteristics of individual drought events are summarized in Table2. The severity of drought events is a function of duration, which is the time period under Isiolo County remains under precipitation deficit. The runs were set to capture the moderate to severely to extremely severe dry events. The spatial extent of the drought characteristics in historical runs are illustrated in figure 7. The locations adjacent to grid points 5 (south) of the study location is adversely affected by frequent (over 75%) and severe droughts lasting for a longer duration (50 months). The interarrival time between two consecutives dry events was also high in these regions. Conversely, the areas around grid points 1 and 2 were less affected by drought

**********Figure 7**********

The most severe dry spell was experienced between March 1983 to March 1988 lasting 61 months followed by the Oct 1998 to Oct 2001 dry spell which lasted for 37 months. The severe droughts peaks captured by the scPDSI runs were February 1981, August 1984, April 1992, June 1994, February 1997, June 2001, July 2011, June 2014. It is evident that there has been a decline in the severity of drought in Isiolo County over the last decade. However it is not clear as to what might be contributing to this shift of events given that recent studies (Dai, 2013a; Ongoma, Chen, et al., 2018) have presented results indicating an increase in the frequencies and severity of the drought events over the larger East African domain.

**********Table 2**********

3.2 Projected Spatial-Temporal Characteristics of Drought using scPDSI based on RCP4.5 and RCP8.5 from CORDEX

Figures 8 and 9 depicts the spatial-temporal characteristics of projected drought patterns are computed using (rainfall and temperature) from the bias corrected CORDEX model simulation

output for the period 2020-2050 based on simple covariant matrix EOF method. ScPDSI was calculated for both RCP 4.5 and RCP 8.5 and objectively analyzed to determine the different aspect of anticipated future dry events based on the run theory. The two leading EOF loadings for RCP 4.5 accounted for 86.1% of the total variability. The first spatial pattern under RCP 4.5 shows and homogenous positive patterns of spatial variability, with the western and eastern sectors of Isiolo County retaining relatively low values. The second EOF loading under RCP4.5 shows both positive and negative spatial variability with more resemblance to EOF2 in figure 5. This depicts that the future dry events are more likely to concentrate on the eastern parts of the County. However, the two-leading spatial EOF loadings for the RCP8.5 both shows both positive and negative spatial patterns with inverted patterns being at the western parts of the County. These patterns show future reduction in drought possibilities over northern parts of the county.

**********Figure 8**********

The temporal evolution of the two leading EOF analysis shows that there is more pronounced interannual variability as compared to interdecadal variability for both dry and wet events. The RCP 4.5 depicts and opposite phase of dry and wet events over the county, however this can be validated by applying theory of runs on the projected originally computed scPDSI values. The average scPDSI over the10 grid points, suggests that there is more of severe dry events over the last decade of the study period for both RCP scenarios.

**********Figure 9**********

The geographical regions extending to the southern zone of the study region along the eastern sides are often defined by bare Arid and Semi-Arid lands. Climate observed in this region are mainly dry with rainfall recorded being below normal climatological averages, resulting in increased evapotranspiration due to increased solar insolation, increased wind speed, and vapor pressure insufficiency, largely associated with higher surface temperatures and low humidity. Intriguingly, zones along the western side may be less impacted by severe drought events. With more vegetation cover, these locations are also high in elevation hence experiences relatively low temperatures.

A summary of the projected dry events and their characteristics detected by the runs are presented in tables 3 and 4 and figures 10 and 11. It is evident that there is a decrease in severity of the projected drought events compared to the historical drought events with only four and two events being identified under RCPs4.5 and 8.5 respectively. The reduction in the severity of the drought events could be linked with the enhance precipitation as revealed by the MK results in this study. RCP4.5 scPDSI shows that Mar 2046 – Mar 2048 is the most severe with dry spell lasting for 25 consecutive months of precipitation deficit. However, RCP8.5 monthly scPDSI runs picks out Nov 2042 – Nov 2046 as the most severe dry spell with a duration of 46 months. The major projected dry events are expected to peak in April 2032, December 2044, December 2046, April 2050.

**********Table 3**********

The spatial distribution of the projected drought characteristics under RCP 4.5 is presented in figure 10. Compared with the historical, there is a shifting increase of severity, frequency and duration to the western and the eastern sides of the county from the central belt. Under RCP8.5 run the western, northern and southern geographical locations are projected to be more adversely impacted by droughts. However, compared with the RCP4.5 there is a general reduction in the severity, frequency and the duration of drought in the results presented.

**********Figure 10**********

**********Table 4**********

**********Figure 11**********

3.3 Projected Drought, Temperature and Rainfall Trends

On running the Mann-Kendall test on the projected scPDSI, both RCP 4.5 and RCP 8.5 temperature and precipitation data, the following results were obtained for the ten grid points in Isiolo and the scPDSI average in Table 5 and 6. If the p-value calculated is less than the threshold level of alpha = 0.05, H_0 is rejected. Rejecting H_0 indicates that the time series has a trend, whereas accepting H_0 indicates that no trend has been detected. On the null rejection, Hypothesis, the outcome is said to be significant statistically.

**********Table 5**********

**********Table 6**********

The spatial trends of the projected droughts are shown in figure 12. These are the Mann-Kendall tau statistics values for each grid points. The result depicts decreasing trends of drought for both RCP4.5 and RCP8.5 simulations. Averaged as in tables 5 and 6 there is a decreasing trend in drought events under RCP4.5 while under RCP8.5 the trends are not statistically significant.

**********Figure 12**********

The sequential Mann-Kendall results at RCP4.5 shows that the forward sequence, u(t) and backward sequence, (u') do not intercept each other until at 2044 where a point of abrupt change is denoted, with the projected trends decreasing significantly. Subsequently, the results of RCP8.5 show that an abrupt change occur earlier ass compared with the RCP4.5. The point of sudden change is detected in 2032 with decreasing drought trends being depicted. The reduction in drought occurrences during the mid-century under the RCP8.5 scenario (Figure 13) is consistent with precipitation predictions that are noted to enhance during the mid-century (Ongoma, Chena, et al., 2018; Shongwe et al., 2009; Spinoni et al., 2020). Previous findings on inter - annual precipitation patterns, especially in the Indian and Pacific Oceans, have shown a significant link between rainfall and SST anomalies (Shongwe et al., 2009; Spinoni et al., 2020). The results presented by these studies concluded that alterations in long-term forcing by greenhouse gas ultimately shifts the SST pattern over the tropical Oceans that generally have a significant feedback relationship with the rainfall variability, thus, affecting drought or flood characteristics.

**********Figure 13**********

Drought occurrence is climatic and/or meteorological event that is mainly driven by fluctuation in hydro-meteorological variables such as precipitation, temperature and soil moisture (Tan et al., 2020). The severity of a drought episode is a factor of precipitation anomalies with prolonged deficits leading into aggravated scenarios (Ayugi et al., 2020a; Dai, 2013a; Spinoni et al., 2020). Therefore, it is critical to study the changes in these hydro-meteorological drivers of drought in order to adequately prepare for actionable contingency measures geared towards drought

mitigation and long-term resilience building. In this study, scPDSI is computed based on RCP 4.5 and RCP8.5 and the projected drought is characterized in order to determine their onset, cessation, severity, duration, geographical extent and intensities which may form a foundation for effective drought management.

After computing the Mann-Kendall statistical test on aerially averaged values of the projected temperature and precipitation data under RCP4.5 and RCP8.5, the following results in Table 7 were obtained for an average for the ten grid points. If the p-value calculated is less than the threshold level of alpha = 0.05, H0 is rejected. Rejecting H0 indicates that the time series has a trend, whereas accepting H0 indicates that no trend has been detected. On the null rejection, Hypothesis, the outcome is said to be significant statistically.

**********Table 7**********

The spatial distribution of the Mann-Kendall tau statistics computed over the individual grid points shows a bi-distribution with both negative and positive trends under RCP4.5 for temperature simulations and homogeneously positive trends for Temperature RCP8.5, Precipitation RCP4.5 and Precipitation RCP8.5. The statistically significant scenario both implies that western parts of the country are likely to be hot and wet. This is mainly affecting the locations with high elevation (next to Mount Kenya).

**********Figure 14**********

The results of the sequential Mann-Kendall statistical test to detect the abrupt change in the temporal time series of temperature and precipitation (figure 15) indicates that although there is changes in the in $u(t)$ and $u^{'}(t)$ for temperature RCP4.5 and precipitation RCP8.5 as shown by the intersections of the forward and backward sequences, the trends are not significant at t statistical test value. The results show a significant change in temporal trends of precipitation at RCP4.5 and temperature at RCP8.5 with both indicating increasing trends occurring from 2043 and 2046 respectively at 95% confidence level.

**********Figure 15**********8

The results of this study concur with other current literature that revealed an increase in the frequency of rainfall over the domain of the study (Ongoma, Chena, et al., 2018). The wetting pattern over the East Africa region was linked by Zhao and Dai (2017) to a strong Indian Ocean ITCZ feedback. Despite the projected future warming, the strong shift denoting the increase in rainfall event concurs with a research by Kent et al. (2015) that identified a lack of causal relationship between global average temperature unpredictability and projected shift in precipitation at the end of the twenty-first century. The study, on the other hand, acknowledged that local precipitation variability over the study region is mainly related to convection and convergence geographic changes, linked with systems such as trends of sea surface temperature (SST) and alteration of land-sea thermal interaction. The inference of numerous studies to clarify the changes in rainfall projections shows the complexity of regional changes in rainfall, resulting majorly to unpredictability about the impact.

4 Conclusion

Drought continues to be one of the most sophisticated climatic phenomena at the global, regional and local levels that impact the economy, environment and society at large. The current study examined drought events by characterizing trends, intensity and severity based on the scPDSI, which is a broadly applied index over Isiolo County, Kenya, on historical and projected scales. Several studies have been done in the wider East African domain to characterize drought patterns based on other index-based drought indicators such as SPI and SPEI (Tan et al., 2020; Ayugi et al., 2020b; Polong et al., 2019; Spinoni et al., 2020). However, these studies have not attempted to address the other factors that affect drought characteristics such as soil characteristics, geographical location among others.

The methodology used in this study is therefore more robust as it includes several variables in self-calibrating the PDSI. Spinoni et al., 2020 while using CORDEX dataset found that at global scale the severity and frequencies under RCP4.5 and RCP8.5 is likely to increase, however in this study, at a smaller scale shows contrary results. In spite of the inconsistency, the common results show that there is more likelihood of a hotter and wetter scenario at local scale as shown in Mann-Kendall results. These results agree with the recent studies (Sheffield et al., 2012; Trenberth et al., 2014) and Inter-governmental Panel Climate Change fifth assessment report that temperature and rainfall are projected to increase. The variation in the drought spatial-temporal

trends may be attributed to the local factors affected droughts that may have not be factored in the projected data such as mesoscale features and synoptic weather patterns such as ENSO and IOD (Ukkola et al. 2018).

The results presented in this study based on EOF analysis shows that scPDSI captured the major historical spatial-temporal characteristics of drought over Isiolo County, Kenya of 1983-1984, 1992-1993, 1999-2000, and 2009-2011 (Balint et al., 2013; Uhe et al., 2018; Wambua et al., 2018) and therefore can be used as an early warning tool to trigger drought emergency response and contingency planning based on the results of the RCP 4.5/8.5 projected drought scenarios. However, this study did not factor in the contribution of human beings in the spatial-temporal characteristics of drought. Thus, this research recommends an in-depth examination on the factor contribution of humans in moderating the projected drought characteristics particularly in the geographical locations that were less impacted by historical droughts. In addition, local drought emergency institutions and government should endeavor to find innovative technologies, mechanism and livelihoods that can cope with excepted impact of drought on food security and natural resource management. This will mitigate society and their livelihoods from the adverse impacts and develop long-term resilience to drought.

Acknowledgements

The first author would like to thank the Kenya Meteorological Department for the study leave accorded to him. Special thanks go to University of Nairobi for providing the required guidance and for all other forms of support. Appreciation goes to the CORDEX and CRU for providing data free of charge.

Compliance with ethical standards

The authors unilaterally certify that there really is no breach of ethics.

Funding Statement

This work was funded by the Kenya Climate Smart Agricultural Project (KCSAP) through the World Bank grant reference KCSAP- WORLD BANK/ IDA Credit P154784.

Author's Contribution

The authors confirm contribution to this paper as follows: study conception and design: Ochieng, P., Nyandega, I.; data collection: Ochieng, P.; analysis and interpretation of results: Ochieng, P.; draft manuscript preparation: Ochieng, P. All authors reviewed the results and approved the final version of the manuscript.

References

Abdulrazzaq, Z. T., Hasan, R. H., & Aziz, N. A. (2019). Integrated TRMM Data and Standardized Precipitation Index to Monitor the Meteorological Drought. *Civil Engineering Journal*, *5*(7), 1590–1598. https://doi.org/10.28991/cej-2019-03091355

AghaKouchak, A. (2015). A multivariate approach for persistence-based drought prediction: Application to the 2010-2011 East Africa drought. *Journal of Hydrology*, *526*, 127–135. https://doi.org/10.1016/j.jhydrol.2014.09.063

Aiguo, D., Kevin, E. T., & Taotao, Q. (2004). A Global Dataset of Palmer Drought Severity Index for 1870 – 2002 : Relationship with Soil Moisture and Effects of Surface Warming. *Journal of Hydrometeorology*, *5*(6), 1117–1130. https://doi.org/10.1016/j.molcel.2017.04.015

Ayugi, B., Tan, G., Rouyun, N., Zeyao, D., Ojara, M., Mumo, L., Babaousmail, H., & Ongoma, V. (2020). Evaluation of meteorological drought and flood scenarios over Kenya, East Africa. *Atmosphere*, *11*(3), 1–22. https://doi.org/10.3390/atmos11030307

Balint, Z., Mutua, F., Muchiri, P., & Omuto, C. T. (2013). Monitoring Drought with the Combined Drought Index in Kenya. In *Developments in Earth Surface Processes* (1st ed., Vol. 16). Elsevier B.V. https://doi.org/10.1016/B978-0-444-59559-1.00023-2

Barua, S., Perera, B. J. C., Ng, A. W. M., & Tran, D. (2010). Drought forecasting using an aggregated drought index and artificial neural network. *Journal of Water and Climate Change*, *1*(3), 193–206. https://doi.org/10.2166/wcc.2010.000

Chen, H., & Sun, J. (2015). Changes in drought characteristics over china using the standardized precipitation evapotranspiration index. *Journal of Climate*, *28*(13), 5430–5447. https://doi.org/10.1175/JCLI-D-14-00707.1

Collaud Coen, M., Andrews, E., Bigi, A., Romanens, G., Martucci, G., & Vuilleumier, L. (2020). Effects of the prewhitening method, the time granularity and the time segmentation on the Mann-Kendall trend detection and the associated Sen's slope. *Atmospheric Measurement Techniques Discussions*, *June*, 1–28. https://doi.org/10.5194/amt-2020-178

Cook, K. H., & Vizy, E. K. (2013). Projected changes in east african rainy seasons. *Journal of Climate*, *26*(16), 5931–5948. https://doi.org/10.1175/JCLI-D-12-00455.1

Dai, A. (2011). Characteristics and trends in various forms of the Palmer Drought Severity Index during 1900-2008. *Journal of Geophysical Research Atmospheres*, *116*(12).

https://doi.org/10.1029/2010JD015541

Dai, A. (2013a). Increasing drought under global warming in observations and models. *Nature Climate Change*, *3*(1), 52–58. https://doi.org/10.1038/nclimate1633

Dai, A. (2013b). The influence of the inter-decadal Pacific oscillation on US precipitation during 1923-2010. *Climate Dynamics*, *41*(3–4), 633–646. https://doi.org/10.1007/s00382-012-1446-5

Dike, V. N., Shimizu, M. H., Diallo, M., Lin, Z., Nwofor, O. K., & Chineke, T. C. (2015). Modelling present and future African climate using CMIP5 scenarios in HadGEM2-ES. *International Journal of Climatology*, *35*(8), 1784–1799. https://doi.org/10.1002/joc.4084

Enfoque, E. L., Monitoreo, D. E. L., Gallego, I., Proyecto Jalda, R. Villalta, A. C., Tapella, E., Gohl, E., Mendoza, R., Melorose, J., Perroy, R., Careas, S., Alianza internacional contra el VIH/SIDA, Centro de Investigación y desarrollo de la educación., María Antonia Rodríguez Arce, Campilan, D., Gaventa, J., Gonsalves, J., Guijt, I., Johnson, D., … Gómez, V. (2010). No Title'거대한 잠재력' 인도·아세안 본격 공략 시동. *International Institute for Environment and Development*, *07/80*(2), 125. https://arxiv.org/pdf/1707.06526.pdf%0Ahttps://www.yrpri.org%0Ahttp://weekly.cnbnews.com/news/article.html?no=124000%0Ahttps://www.fordfoundation.org/%0Ahttp://bibliotecavirtual.clacso.org.ar/Republica_Dominicana/ccp/20120731051903/prep%0Ahttp://webpc.cia

Fernando, S., Xavier, A., Jale, S., Stosic, T., Antonio, C., & Singh, V. P. (2020). *Precipitation Trends Analysis by Mann-Kendall Test : A Case Study of Análise de Tendência da Precipitação Usando o Teste de Mann-Kendall : Um Estudo de Caso na Paraíba , Brasil*. *2012*, 187–196.

Funk, C.; Peterson, P.; Landsfeld, M.; Pedreros, D.; Verdin, J.; Shukla, S.; Michaelsen, J., 2015. The climate hazards infrared precipitation with stations—A new environmental record for monitoring extremes. Sci. Data, 2, 150066.

Funk, C., Dettinger, M. D., Michaelsen, J. C., Verdin, J. P., Brown, M. E., Barlow, M., & Hoell, A. (2008). Warming of the Indian Ocean threatens eastern and southern African food security but could be mitigated by agricultural development. *Proceedings of the National Academy of Sciences of the United States of America*, *105*(32), 11081–11086. https://doi.org/10.1073/pnas.0708196105

Funk, C., Eilerts, G., Davenport, F., & Michaelsen, J. (2010). A Climate Trend Analysis of

Kenya-August 2010. *Famine Early Warning Systems Network-Informing Climate Change Adaptation Series*, *1975*(August), 1–4. http://fews.net/sites/default/files/documents/reports/fs2010-3074.pdf

Gadedjisso-Tossou, A., Adjegan, K. I., & Kablan, A. K. M. (2020). Rainfall and Temperature Trend Analysis by Mann–Kendall Test and Significance for Rainfed Cereal Yields in Northern Togo. *Sci*, *2*(4), 74. https://doi.org/10.3390/sci2040074

Gavrilov, M. B., Marković, S. B., Janc, N., Nikolić, M., Valjarević, A., Komac, B., Zorn, M., Punišić, M., & Bačević, N. (2018). Assessing average annual air temperature trends using the Mann–Kendall test in Kosovo. *Acta Geographica Slovenica*, *58*(1 Special Issue), 7–25. https://doi.org/10.3986/AGS.1309

Hao, Z., & AghaKouchak, A. (2013). Multivariate Standardized Drought Index: A parametric multi-index model. *Advances in Water Resources*, *57*, 12–18. https://doi.org/10.1016/j.advwatres.2013.03.009

Hao, Z., Singh, V. P., & Xia, Y. (2018). Seasonal Drought Prediction: Advances, Challenges, and Future Prospects. *Reviews of Geophysics*, *56*(1), 108–141. https://doi.org/10.1002/2016RG000549

Hayes, M. J., Svoboda, M. D., Wilhite, D. A., & Vanyarkho, O. V. (1999). Monitoring the 1996 Drought Using the Standardized Precipitation Index. *Bulletin of the American Meteorological Society*, *80*(3), 429–438. https://doi.org/10.1175/1520-0477(1999)080<0429:MTDUTS>2.0.CO;2

Harris, I.; Jones, P.D.; Osborn, T.J.; Lister, D.H., 2014. Updated high-resolution grids of monthly climatic observations–the CRU TS3.10 Dataset. Int. J. Climatol. 34, 623–642.

Hu, Z., Liu, S., Zhong, G., Lin, H., & Zhou, Z. (2020). Modified Mann-Kendall trend test for hydrological time series under the scaling hypothesis and its application. *Hydrological Sciences Journal*, *65*(14), 2419–2438. https://doi.org/10.1080/02626667.2020.1810253

Huang, J., Yu, H., Guan, X., Wang, G., & Guo, R. (2015). *Accelerated dryland expansion under climate change*. *October*. https://doi.org/10.1038/NCLIMATE2837

Huang, S., Huang, Q., & Leng, G. (2016). *Linkages between hydrological drought , climate indices and human activities : a case study in the Columbia River basin*. *290*(April 2015), 280–290. https://doi.org/10.1002/joc.4344

Huang, S., Huang, Q., Leng, G., & Liu, S. (2016). A nonparametric multivariate standardized drought index for characterizing socioeconomic drought : A case study in the Heihe River

Basin A nonparametric multivariate standardized drought index for characterizing socioeconomic drought : A case study in the. *Journal of Hydrology*, *542*(September), 875–883. https://doi.org/10.1016/j.jhydrol.2016.09.059

Kalisa, W., Zhang, J., Igbawua, T., Ujoh, F., Ebohon, O. J., Namugize, J. N., & Yao, F. (2020). Spatio-temporal analysis of drought and return periods over the East African region using Standardized Precipitation Index from 1920 to 2016. *Agricultural Water Management*, *237*(April), 106195. https://doi.org/10.1016/j.agwat.2020.106195

Karanja, A., Ondimu, K., & Recha, C. (2017). *Analysis of Temporal Drought Characteristic Using SPI Drought Index Based on Rainfall Data in Laikipia West Sub-County , Kenya*. *4*, 1–12. https://doi.org/10.4236/oalib.1103765

Karmeshu Supervisor Frederick Scatena, N. N. (2015). Trend Detection in Annual Temperature & Precipitation using the Mann Kendall Test – A Case Study to Assess Climate Change on Select States in the Northeastern United States. *Mausam*, *66*(1), 1–6. http://repository.upenn.edu/mes_capstones/47

Kumar, N., Panchal, C. C., Chandrawanshi, S. K., & Thanki, J. D. (2017). Analysis of rainfall by using Mann-Kendall trend, sen's slope and variability at five districts of south Gujarat, India. *Mausam*, *68*(2), 205–222.

Le, P. V. V., Phan-Van, T., Mai, K. V., & Tran, D. Q. (2019). Space–time variability of drought over Vietnam. *International Journal of Climatology*, *39*(14), 5437–5451. https://doi.org/10.1002/joc.6164

Leasor, Z. T., Quiring, S. M., & Svoboda, M. D. (2020). Utilizing objective drought severity thresholds to improve drought monitoring. *Journal of Applied Meteorology and Climatology*, *59*(3), 455–475. https://doi.org/10.1175/JAMC-D-19-0217.1

Lin, W., Wen, C., & Wen, Z. (2014). *Assessment of Future Drought in Southwest China Based on CMIP5 Multimodel Projections Assessment of Future Drought in Southwest China Based on CMIP5 Multimodel Projections*. *September*. https://doi.org/10.1007/s00376-014-3223-3

Lorenz E N (1956).Empirical orthogonal functions and statistical weather prediction. Sci Rep No.1,M.I.T Statistical Forecasting Project,contract no. AF19(604)

M. Huho, J., & Kosonei, R. C. (2014). Understanding Extreme Climatic Events for Economic Development in Kenya. *IOSR Journal of Environmental Science, Toxicology and Food Technology*, *8*(2), 14–24. https://doi.org/10.9790/2402-08211424

M Wambua, R. (2014). Drought Forecasting Using Indices and Artificial Neural Networks for Upper Tana River Basin, Kenya-A Review Concept. *Journal of Civil & Environmental Engineering*, *04*(04). https://doi.org/10.4172/2165-784x.1000152

Malakiya, A. D., & Suryanarayana, T. M. V. (2013). Assessment of Drought Using Standardized Precipitation Index (SPI) and Reconnaissance Drought Index (RDI): A Case Study of Amreli District. *International Journal of Science and Research*, *5*(8), 2319–7064.

622 Masupha, T. E., & Moeletsi, M. E. (2017). Use of standardized precipitation evapotranspiration
623 index to investigate drought relative to maize, in the Luvuvhu River catchment area, South
624 Africa. *Physics and Chemistry of the Earth*, *102*, 1–9.
625 https://doi.org/10.1016/j.pce.2017.08.002

626 Mckee, T. B., Doesken, N. J., & Kleist, J. (1993). *The relationship of drought frequency and*
627 *duration to time scales*. *January*, 17–22.

628 Mishra, A. K., & Singh, V. P. (2010a). A review of drought concepts. *Journal of Hydrology*,
629 *391*(1–2), 202–216. https://doi.org/10.1016/j.jhydrol.2010.07.012

630 Mishra, A. K., & Singh, V. P. (2010b). Review paper A review of drought concepts. *JOURNAL*
631 *OF HYDROLOGY*. https://doi.org/10.1016/j.jhydrol.2010.07.012

632 Mishra, A. K., & Singh, V. P. (2011). Drought modeling - A review. *Journal of Hydrology*,
633 *403*(1–2), 157–175. https://doi.org/10.1016/j.jhydrol.2011.03.049

634 Mutsotso, R. B., Sichangi, A. W., & Makokha, G. O. (2018). *Spatio-Temporal Drought*
635 *Characterization in Kenya from 1987 to 2016*. 125–143.
636 https://doi.org/10.4236/ars.2018.72009

637 Ngozi Isioma, I. (2018). Non-parametric Mann-Kendall Test Statistics for Rainfall Trend
638 Analysis in Some Selected States within the Coastal Region of Nigeria. *Journal of Civil,*
639 *Construction and Environmental Engineering*, *3*(1), 17.
640 https://doi.org/10.11648/j.jccee.20180301.14

641 Nikzad Tehrani, E., Sahour, H., & Booij, M. J. (2019). Trend analysis of hydro-climatic
642 variables in the north of Iran. *Theoretical and Applied Climatology*, *136*(1–2), 85–97.
643 https://doi.org/10.1007/s00704-018-2470-0

644 Oguntunde, P. G., Abiodun, B. J., & Lischeid, G. (2017). Impacts of climate change on hydro-
645 meteorological drought over the Volta Basin, West Africa. *Global and Planetary Change*,
646 *155*(July), 121–132. https://doi.org/10.1016/j.gloplacha.2017.07.003

647 Omondi, O. A. (2014). *Analysis of Meteorological Drought in North Eastern Province of Kenya*
648 *Earth Science & Climatic Change Analysis of Meteorological Drought in North Eastern*
649 *Province of Kenya*. *September*. https://doi.org/10.4172/2157-7617.1000219

650 Ongoma, V., Chen, H., Gao, C., Nyongesa, A. M., & Polong, F. (2018). Future changes in
651 climate extremes over Equatorial East Africa based on CMIP5 multimodel ensemble.
652 *Natural Hazards*, *90*(2), 901–920. https://doi.org/10.1007/s11069-017-3079-9

653 Ongoma, V., Chena, H., & Gaoa, C. (2018). Projected changes in mean rainfall and temperature
654 over east Africa based on CMIP5 models. *International Journal of Climatology*, *38*(3),
655 1375–1392. https://doi.org/10.1002/joc.5252

656 Ood, E. R. I. C. F. W. (2008). *Global Trends and Variability in Soil Moisture and Drought*
657 *Characteristics , 1950 – 2000 , from Observation-Driven Simulations of the Terrestrial*

Hydrologic Cycle. *Wang 2003*, 432–458. https://doi.org/10.1175/2007JCLI1822.1

Owiti Zablone, Ogallo Laban, & Mutemi Joseph. (2008). Linkages between the Indian Ocean Dipole and east African seasonal rainfall anomalies. *Journal of the Kenya Meteorological Society*, *2*(2), 2–17. www.kenyamet.org

Palmer, W. C. (1965). Meteorological Drought. In *U.S. Weather Bureau, Res. Pap. No. 45* (p. 58). https://www.ncdc.noaa.gov/temp-and-precip/drought/docs/palmer.pdf

Polong, F., Chen, H., Sun, S., & Ongoma, V. (2019). Temporal and spatial evolution of the standard precipitation evapotranspiration index (SPEI) in the Tana River Basin, Kenya. *Theoretical and Applied Climatology*, *138*(1–2), 777–792. https://doi.org/10.1007/s00704-019-02858-0

Quandt, A., & Kimathi, Y. A. (2016). Adapting livelihoods to floods and droughts in arid Kenya: Local perspectives and insights. *African Journal of Rural Development*, *1*(1), 51–60.

Quiring, S. M. (2009). *Monitoring Drought : An Evaluation of Meteorological Drought Indices*. *1*, 64–88.

Quiring, S. M., & Ganesh, S. (2010). *Agricultural and Forest Meteorology Evaluating the utility of the Vegetation Condition Index (VCI) for monitoring meteorological drought in Texas*. *150*, 330–339. https://doi.org/10.1016/j.agrformet.2009.11.015

Rahman, M. A., Yunsheng, L., & Sultana, N. (2017). Analysis and prediction of rainfall trends over Bangladesh using Mann–Kendall, Spearman's rho tests and ARIMA model. *Meteorology and Atmospheric Physics*, *129*(4), 409–424. https://doi.org/10.1007/s00703-016-0479-4

Rahman, M. R., & Lateh, H. (2016). Meteorological drought in Bangladesh: assessing, analysing and hazard mapping using SPI, GIS and monthly rainfall data. *Environmental Earth Sciences*, *75*(12). https://doi.org/10.1007/s12665-016-5829-5

Rauf, A. U., Rafi, M. S., Ali, I., & Muhammad, U. W. (2016). Temperature trend detection in upper Indus basin by using Mann-Kendall test. *Advances in Science, Technology and Engineering Systems*, *1*(4), 5–13. https://doi.org/10.25046/aj010402

Richard, Y., Fauchereau, N., Poccard, I., Rouault, M., & Trzaska, S. (2001). *20th CENTURY DROUGHTS IN SOUTHERN AFRICA : SPATIAL AND TEMPORAL VARIABILITY , TELECONNECTIONS WITH OCEANIC AND ATMOSPHERIC CONDITIONS*. *885*, 873–885.

Rosenzweig, C. E., & Ridge, O. (1986). *Global Soil Texture and Derived Water-Holding Capacities (Webb et al .) Summary : References : Data Format : Document Information :* https://doi.org/10.3334/ORNLDAAC/548.References

Sa'adi, Z., Shahid, S., Ismail, T., Chung, E. S., & Wang, X. J. (2019). Trends analysis of rainfall and rainfall extremes in Sarawak, Malaysia using modified Mann–Kendall test. *Meteorology and Atmospheric Physics*, *131*(3), 263–277. https://doi.org/10.1007/s00703-017-0564-3

696 Salami, A. W., Ikpee, O. D., Ibitoye, A. B., & Oritola, S. F. (2016). Trend analysis of hydro-
697 meteorological variables in the coastal area of Lagos using Mann-Kendall trend and
698 Standard Anomaly Index methods. *Journal of Applied Sciences and Environmental*
699 *Management*, *20*(3), 797. https://doi.org/10.4314/jasem.v20i3.34

700 Sayyad, R. S., Dakhore, K. K., & Phad, S. V. (2019). Analysis of rainfall trend of Parbhani ,
701 Maharshtra using Mann – Kendall test. *Journal of Agrometeorology*, *21*(2), 239–240.

702 Schilling, J., Opiyo, F. E. O., & Scheffran, J. (2012). *Raiding pastoral livelihoods : motives and*
703 *effects of violent conflict in north-western Kenya*. *KNBS 2010*, 1–16.

704 Schrier, G. Van Der, Barichivich, J., Briffa, K. R., & Jones, P. D. (2013). *A scPDSI-based global*
705 *data set of dry and wet spells for 1901 – 2009*. *118*(July 2012), 4025–4048.
706 https://doi.org/10.1002/jgrd.50355

707 Sharma, D., Kumar, B., & Chand, S. (2019). A Trend Analysis of Machine Learning Research
708 with Topic Models and Mann-Kendall Test. *International Journal of Intelligent Systems*
709 *and Applications*, *11*(2), 70–82. https://doi.org/10.5815/ijisa.2019.02.08

710 Sharma, S., Ranjeet, Dubey, P., Mirdha, I. S., & Sikarwar, R. S. (2018). Precipitation Trend
711 Analysis by Mann-Kendall Test of Different Districts of Malwa Agroclimatic Zone
712 Precipitation Trend Analysis by Mann-Kendall Test of Different Districts of Malwa
713 Agroclimatic Zone. *Environment and Ecology*, *36*(2A), 664–671.

714 Sheffield, J., Wood, E. F., & Roderick, M. L. (2012). Little change in global drought over the
715 past 60 years. *Nature*, *491*(7424), 435–438. https://doi.org/10.1038/nature11575

716 Shimizu, M. H. (2015). *MJO influence on ENSO effects in precipitation and temperature over*
717 *South America*. *March*. https://doi.org/10.1007/s00704-015-1421-2

718 Shongwe, M. E., Oldenborgh, G. J. Van, Nederlands, K., Instituut, M., Nederlands, K., &
719 Instituut, M. (2009). *Projected Changes in Mean and Extreme Precipitation in Africa under*
720 *Global Warming . Part II : East Africa Global Warming . Part II : East Africa*. *April 2016*.
721 https://doi.org/10.1175/2010JCLI2883.1

722 Sneyers R. (1990). On the statistical analysis of series of observations, Tech. Note 143, WMO-
723 No. 415, 192.

724 Spinoni, J., Barbosa, P., Bucchignani, E., Cassano, J., Cavazos, T., Christensen, J. H.,
725 Christensen, O. B., Coppola, E., Evans, J., Geyer, B., Giorgi, F., Hadjinicolaou, P., Jacob,
726 D., Katzfey, J., Koenigk, T., Laprise, R., Lennard, C. J., Kurnaz, M. L., Delei, L. I., …
727 Dosio, A. (2020). Future global meteorological drought hot spots: A study based on
728 CORDEX data. *Journal of Climate*, *33*(9), 3635–3661. https://doi.org/10.1175/JCLI-D-19-
729 0084.1

730 Sridhar, S. ., & Raviraj, A. (2017). Statistical Trend Analysis of Rainfall in Amaravathi River
731 Basin using Mann-Kendall Test. *Current World Environment*, *12*(1), 89–96.
732 https://doi.org/10.12944/cwe.12.1.11

733 Svoboda, M. D., Fuchs, B. A., Poulsen, C. C., & Nothwehr, J. R. (2015). The drought risk atlas:

Enhancing decision support for drought risk management in the United States. *Journal of Hydrology*, *526*, 274–286. https://doi.org/10.1016/j.jhydrol.2015.01.006

Svoboda, M., & Fuchs, B. (2016). *Handbook of Drought Indicators and Indices Handbook of Drought Indicators and Indices*.

Tan, G., Ayugi, B., Ngoma, H., & >Ongoma, V. (2020). Projections of future meteorological drought events under representative concentration pathways (RCPs) of CMIP5 over Kenya, East Africa. *Atmospheric Research*, *246*(July), 105112. https://doi.org/10.1016/j.atmosres.2020.105112

Tatl, H. (2009). *Use of the standardized precipitation index (SPI) and a modified SPI for shaping the drought probabilities over Turkey †*. *2282*(February), 2270–2282. https://doi.org/10.1002/joc

Technische Universtität München, L.-M.-U. M. (2018). 済無No Title No Title. *E-Conversion - Proposal for a Cluster of Excellence*.

Tesso, G., Emana, B., & Ketema, M. (2012). Analysis of vulnerability and resilience to climate change induced shocks in North Shewa, Ethiopia. *Agricultural Sciences*, *03*(06), 871–888. https://doi.org/10.4236/as.2012.36106

Thenmozhi, M., & Kottiswaran, S. V. (2016). Analysis of Rainfall Trend Using Mann – Kendall Test and the Sen ' S. *International Journal of Agricultural Science and Research*, *6*(2), 131–138.

Tierney, J. E., Ummenhofer, C. C., & Peter, B. (2015). *Past and future rainfall in the Horn of Africa*. *October*, 1–9.

Tirivarombo, S., Osupile, D., & Eliasson, P. (2018). Drought monitoring and analysis: Standardised Precipitation Evapotranspiration Index (SPEI) and Standardised Precipitation Index (SPI). *Physics and Chemistry of the Earth*, *106*, 1–10. https://doi.org/10.1016/j.pce.2018.07.001

Trenberth, K. E., Dai, A., Schrier, G. Van Der, Jones, P. D., Barichivich, J., Briffa, K. R., & Sheffield, J. (2014). *Global warming and changes in drought*. *4*(December 2013), 3–8. https://doi.org/10.1038/NCLIMATE2067

Tsakiris, G., Tigkas, D., Vangelis, H., & Pangalou, D. (2007). *CHAPTER 9 REGIONAL DROUGHT IDENTIFICATION AND ASSESSMENT . CASE STUDY IN CRETE*. 169–170.

Tschirley, D., Arlindo, P., Nijhoff, J. J., Mwinga, B., Weber, M. T., & Jayne, T. S. (2005). *Learning from the 2002/03 Food Crisis in Southern Africa: Lessons for the Current Year *. *46*, 1–4.

Uhe, P., Philip, S., Kew, S., Shah, K., Kimutai, J., Mwangi, E., van Oldenborgh, G. J., Singh, R., Arrighi, J., Jjemba, E., Cullen, H., & Otto, F. (2018). Attributing drivers of the 2016 Kenyan drought. *International Journal of Climatology*, *38*(December 2017), e554–e568. https://doi.org/10.1002/joc.5389

Vogel, C., Koch, I., & Van Zyl, K. (2010). "A persistent truth"-reflections on drought risk management in Southern Africa. *Weather, Climate, and Society*, *2*(1), 9–22. https://doi.org/10.1175/2009WCAS1017.1

Wambua, Raphael M, Mutua, B. M., & Raude, J. M. (2018). *Detection of Spatial , Temporal and Trend of Meteorological Drought Using Standardized Precipitation Index (SPI) and Effective Drought Index (EDI) in the Upper Tana River Basin , Kenya*. 83–100. https://doi.org/10.4236/ojmh.2018.83007

Wilhite, D A. (2011). *Breaking the Hydro-Illogical Cycle : Progress or Status Quo for Drought Management in the United States*. 5–18.

Wilhite, Donald A, Svoboda, M. D., & Hayes, M. J. (2007). *Understanding the Complex Impacts of Drought : A Key to Enhancing Drought Mitigation and Preparedness Understanding the Complex Impacts of Drought : A Key to Enhancing Drought Mitigation and Preparedness*. https://doi.org/10.1007/s11269-006-9076-5.Copyright

Xing, L., Huang, L., Chi, G., Yang, L., Li, C., & Hou, X. (2018). A dynamic study of a karst spring based on wavelet analysis and the Mann-Kendall trend test. *Water (Switzerland)*, *10*(6). https://doi.org/10.3390/w10060698

Yan, H., Wang, S., Lu, H., Yu, Q., Zhu, Z., Myneni, R. B., Liu, Q., & Shugart, H. H. (2014). *Journal of Geophysical Research : Atmospheres*. 9419–9440. https://doi.org/10.1002/2014JD021673.Received

Yevjevich, V. (1969). An objective approach to definitions and investigations of continental hydrologic droughts. *Journal of Hydrology*, *7*(3), 353. https://doi.org/10.1016/0022-1694(69)90110-3

Yilmaz, B. (2019). Analysis of hydrological drought trends in the GAP region (southeastern Turkey) by Mann-Kendall test and innovative sen method. *Applied Ecology and Environmental Research*, *17*(2), 3325–3342. https://doi.org/10.15666/aeer/1702_33253342

Yu, M. (2014). *Are droughts becoming more frequent or severe in China based on the Standardized Precipitation Evapotranspiration Index : 1951 – 2010 ? 558*(May 2013), 545–558. https://doi.org/10.1002/joc.3701

Zablone, O., & Ogalo, L. (2014). *Linkages between the Indian Ocean Dipole and East African Rainfall Anomalies Linkages between the Indian Ocean Dipole and East African Seasonal Rainfall Anomalies*. *July*, 2–17.

Zargar, A., Sadiq, R., Naser, B., & Khan, F. I. (2004). *A review of drought indices*. https://doi.org/10.1139/A11-013

Zhang, Y., Cabilio, P., & Nadeem, K. (2016). Improved seasonal mann–kendall tests for trend analysis in water resources time series. *Fields Institute Communications*, *78*(January 2018), 215–229. https://doi.org/10.1007/978-1-4939-6568-7_10

Zhao, T., Dai, A., 2017. Uncertainties in historical changes and future projections of drought.

Part II: model-simulated historical and future drought changes. Clim. Chang. 144, 535–548. https://doi.org/10.1007/s10584-016-1742-x.

Zhong, L., Liu, L., & Liu, Y. (2010). *International Conference on Agricultural Risk and Food Security 2010 Natural Disaster Risk Assessment of Grain Production in Dongting Lake Area , China*. *1*, 24–32. https://doi.org/10.1016/j.aa

Figures

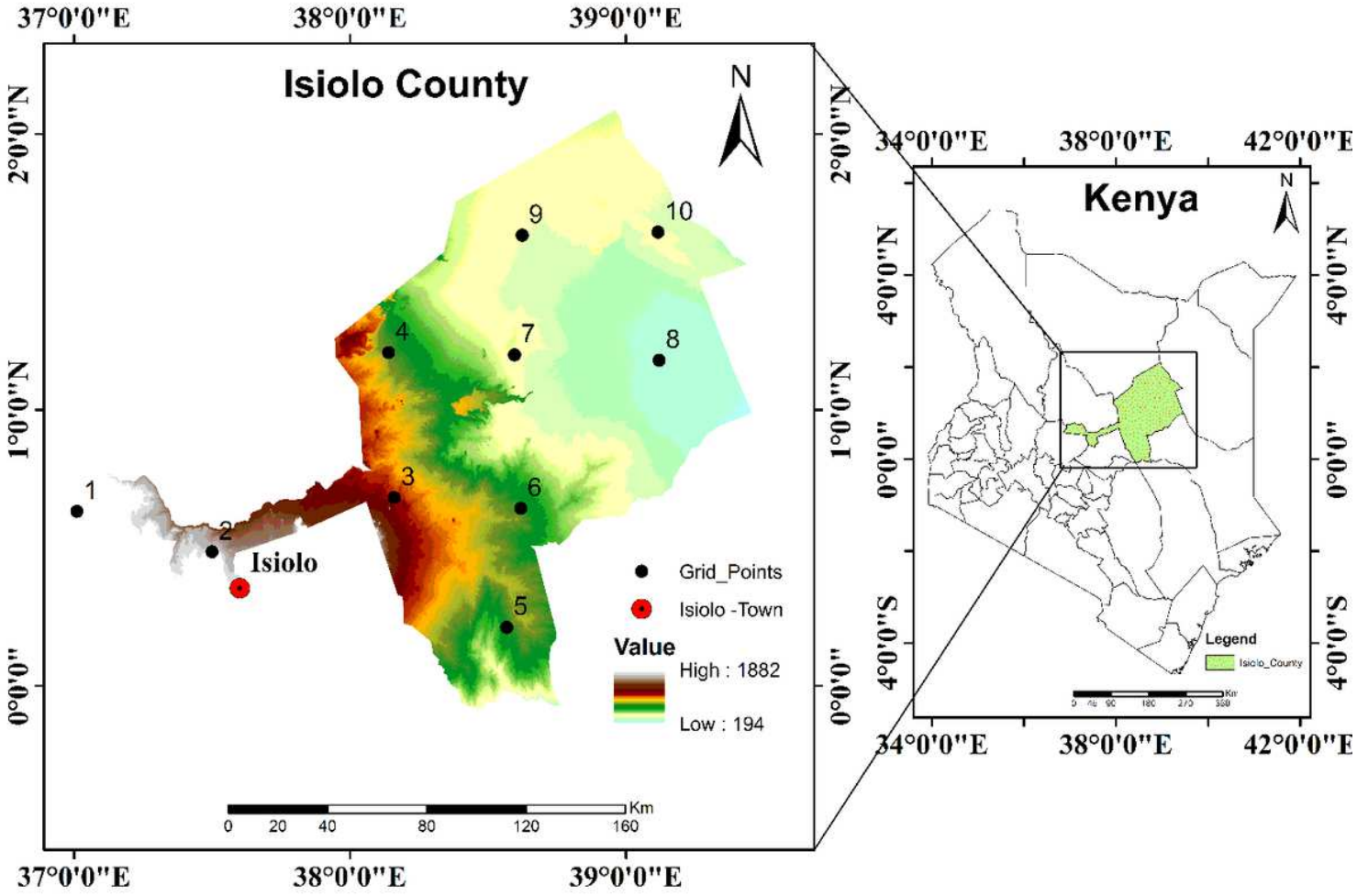

Figure 1

Location of study area

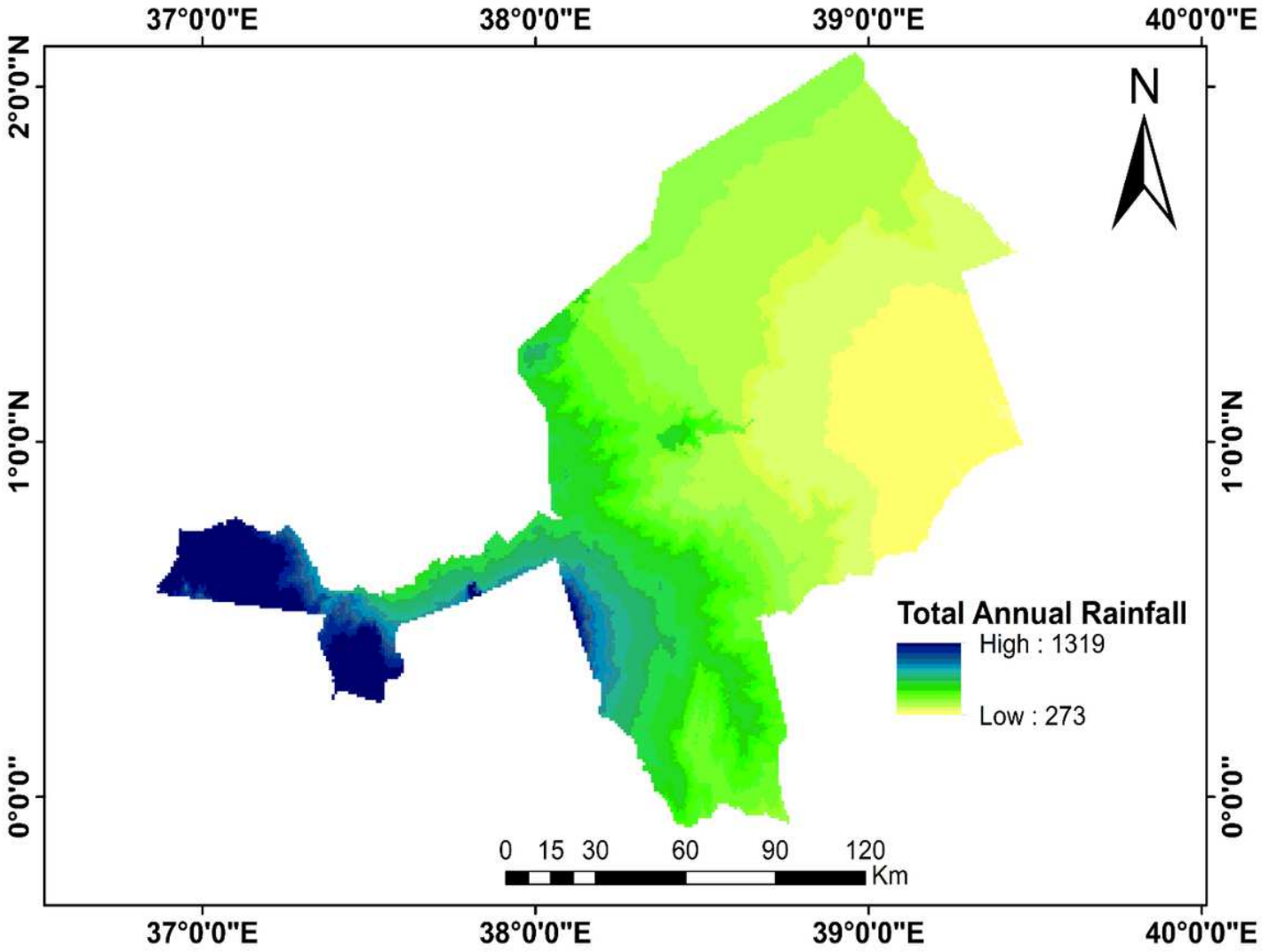

Figure 2

Mean annual Rainfall (mm/year) distribution in Isiolo County, Kenya

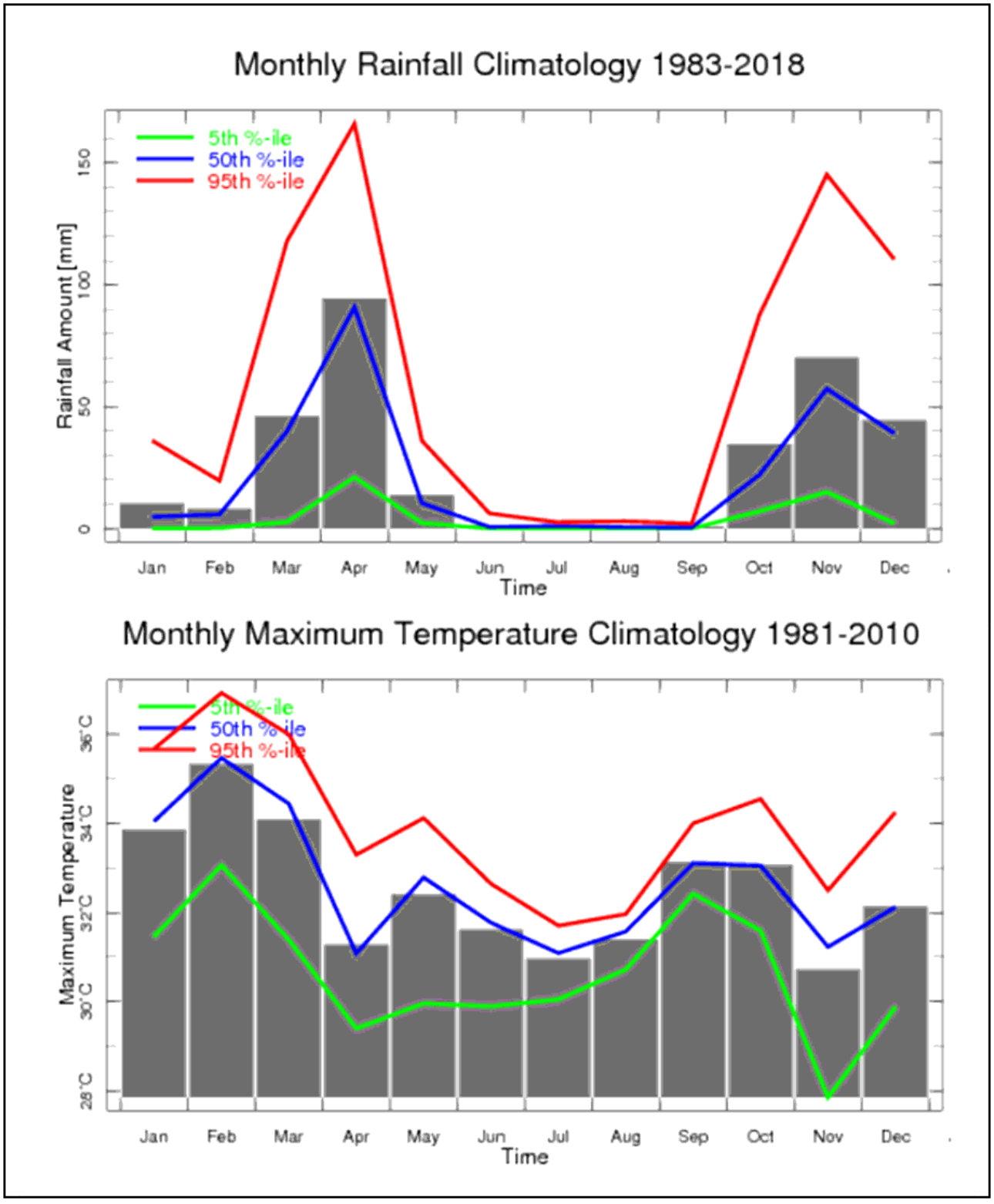

Figure 3

Annual Rainfall (mm/Month) and temperature (oC/Month) cycles top panel and bottom panels respectively over Isiolo County, Kenya

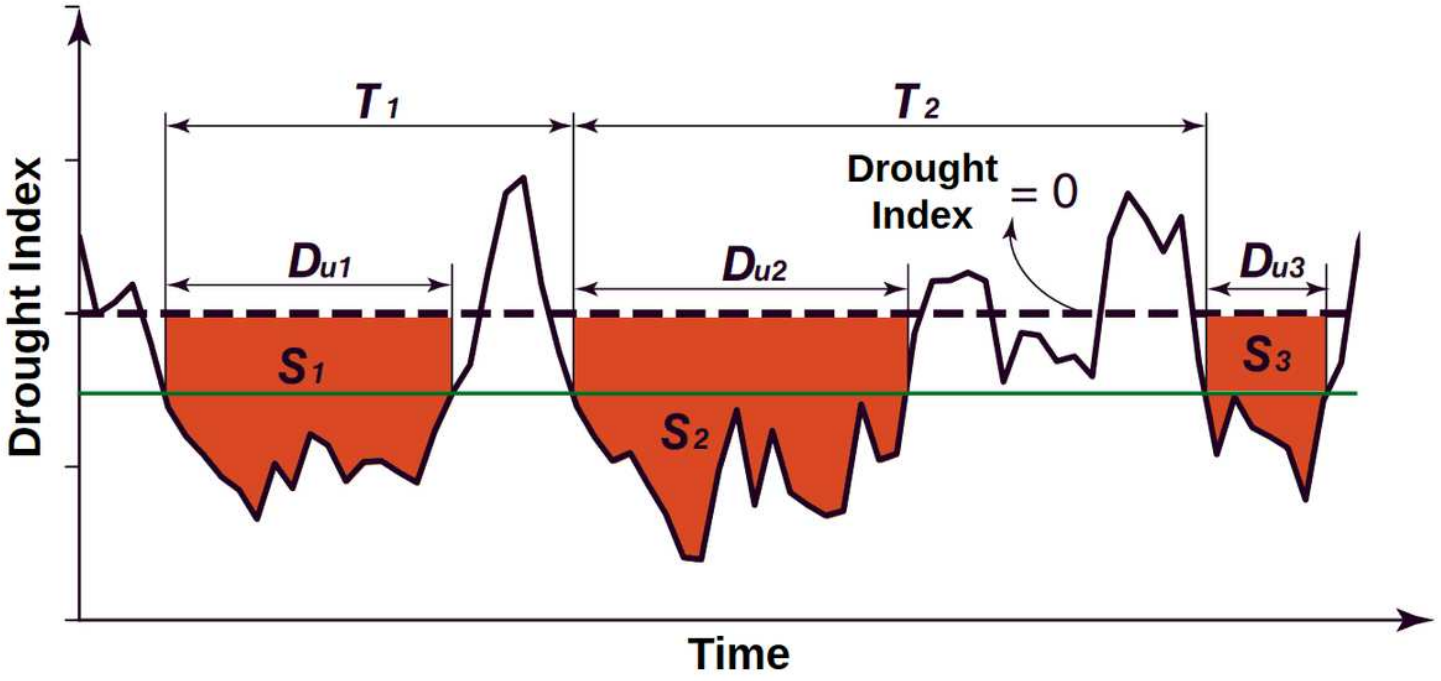

Figure 4

Illustration of drought events and characteristics

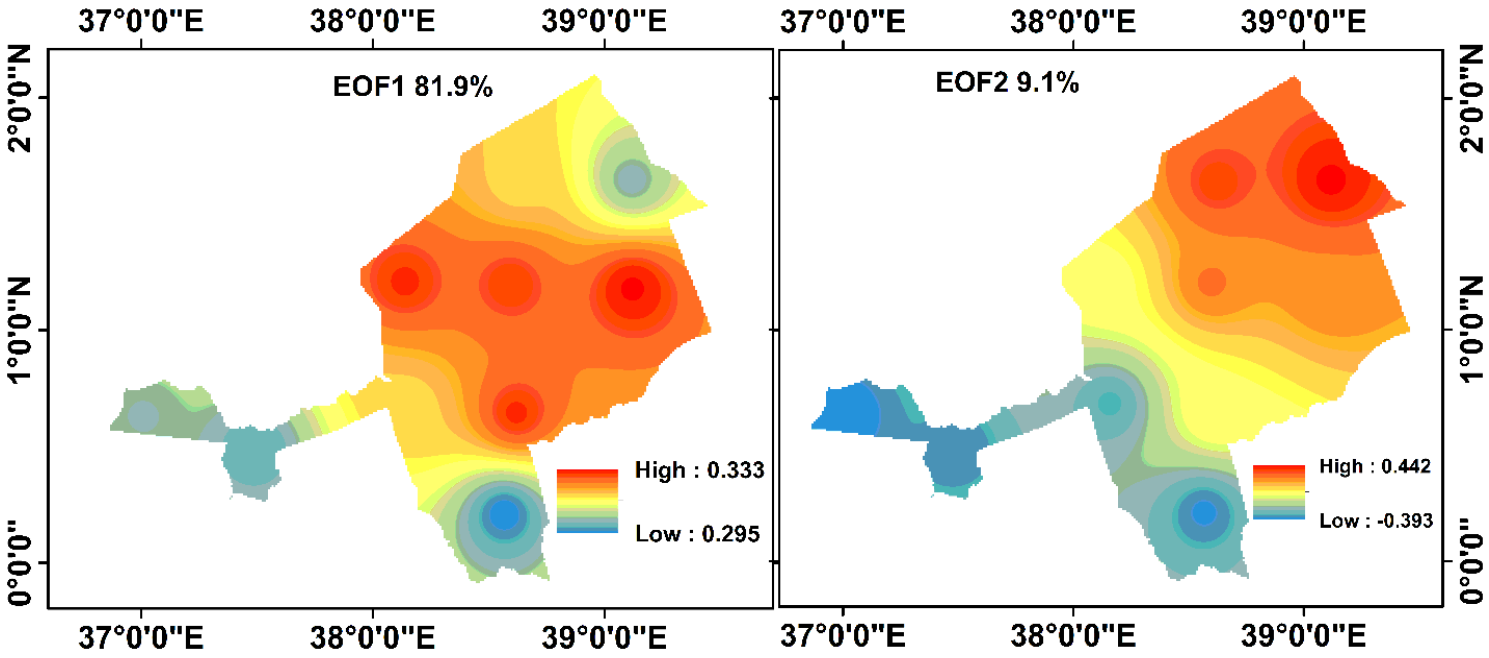

Figure 5

Spatial patterns of first two dominant EOF loadings for historical (1980-2018) scPDSI in Isiolo County, Kenya

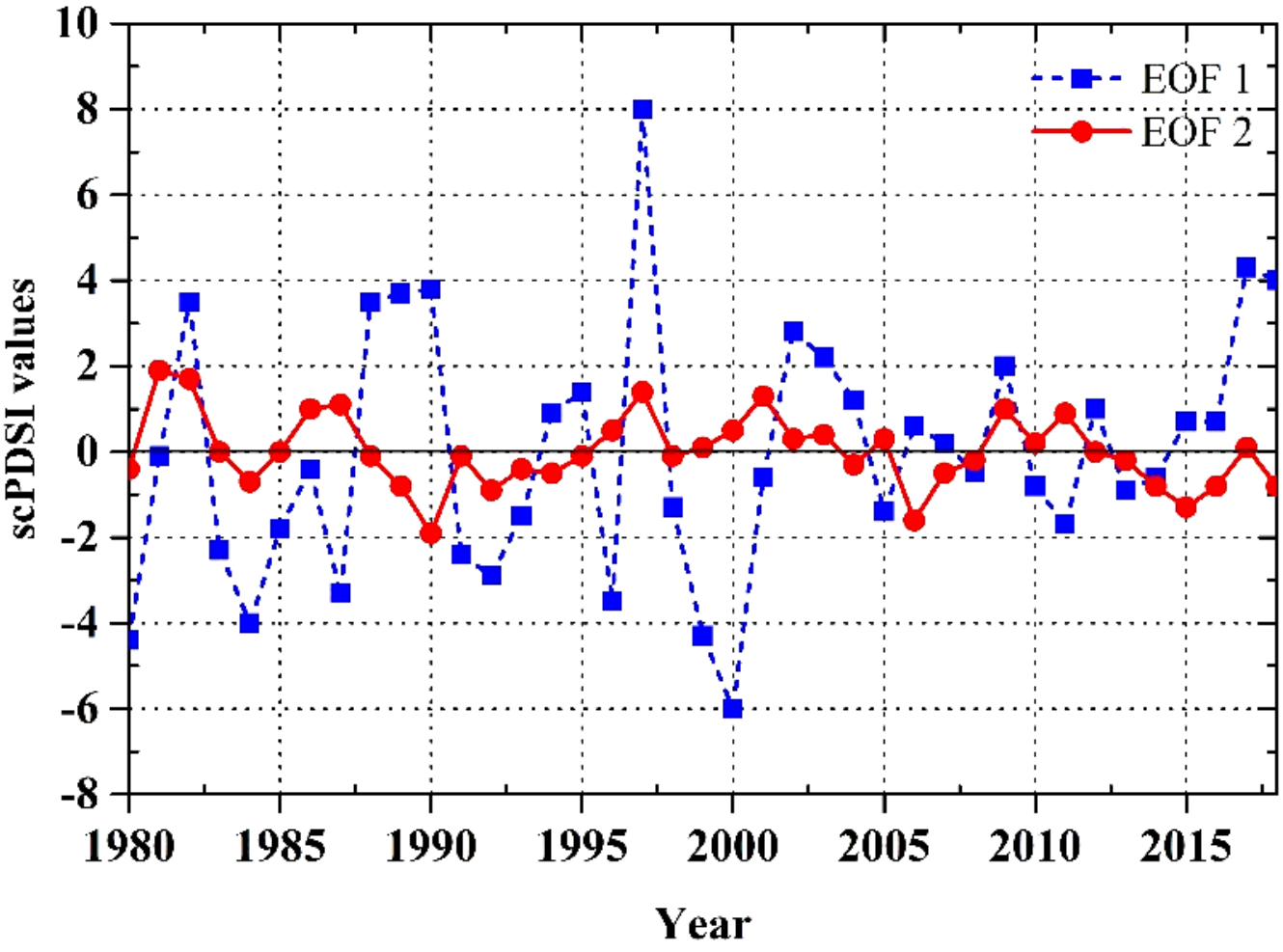

Figure 6

The temporal pattern of EOF scores corresponding to the first two dominant loading for historical (1980-2018) scPDSI

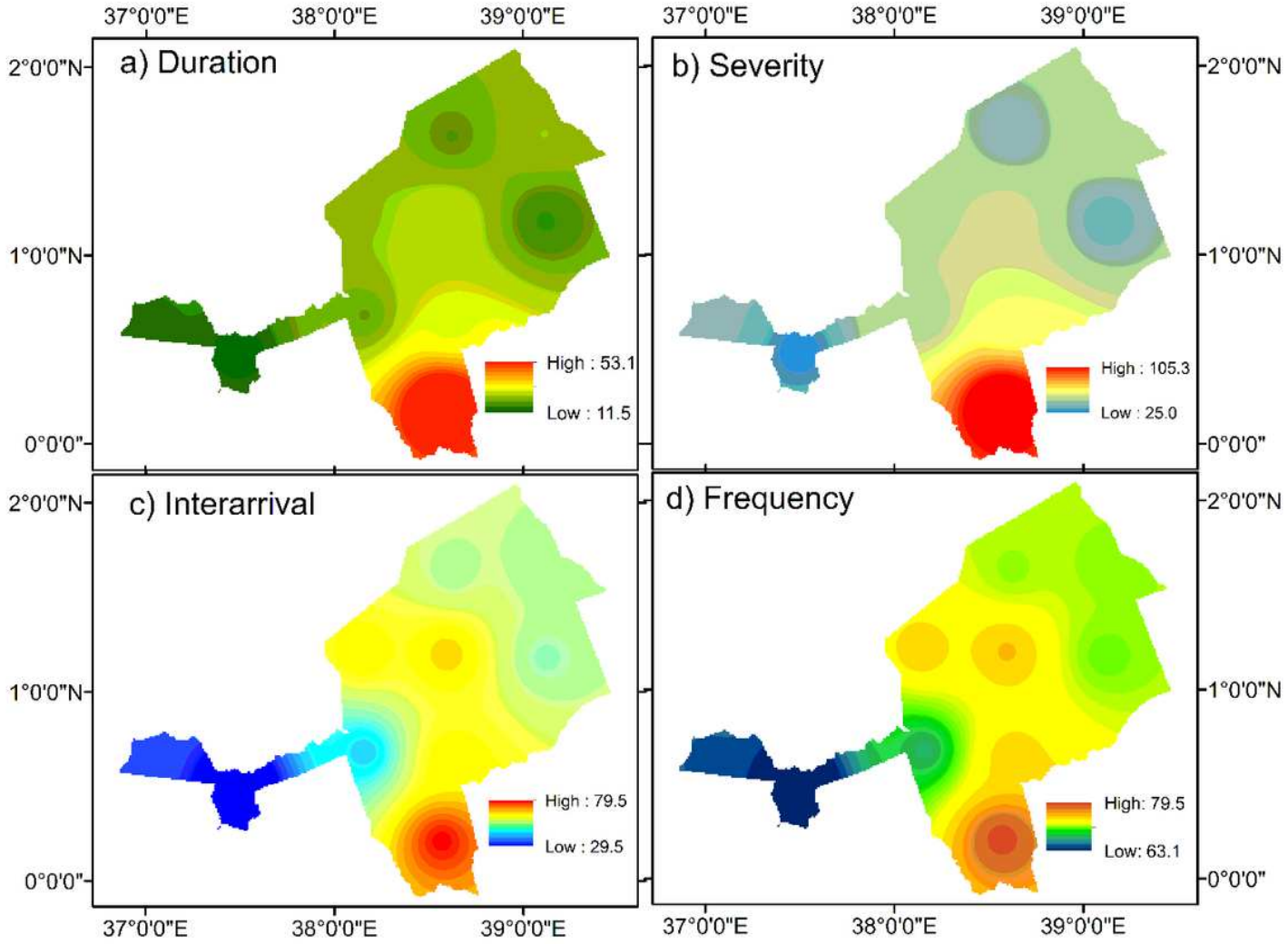

Figure 7

Historical (1980-2018) drought characteristics based on run theory (scPDSI ≤ - 1). a) Duration (Months), b) Severity c) Interarrival (Months) and d) Frequency (%)

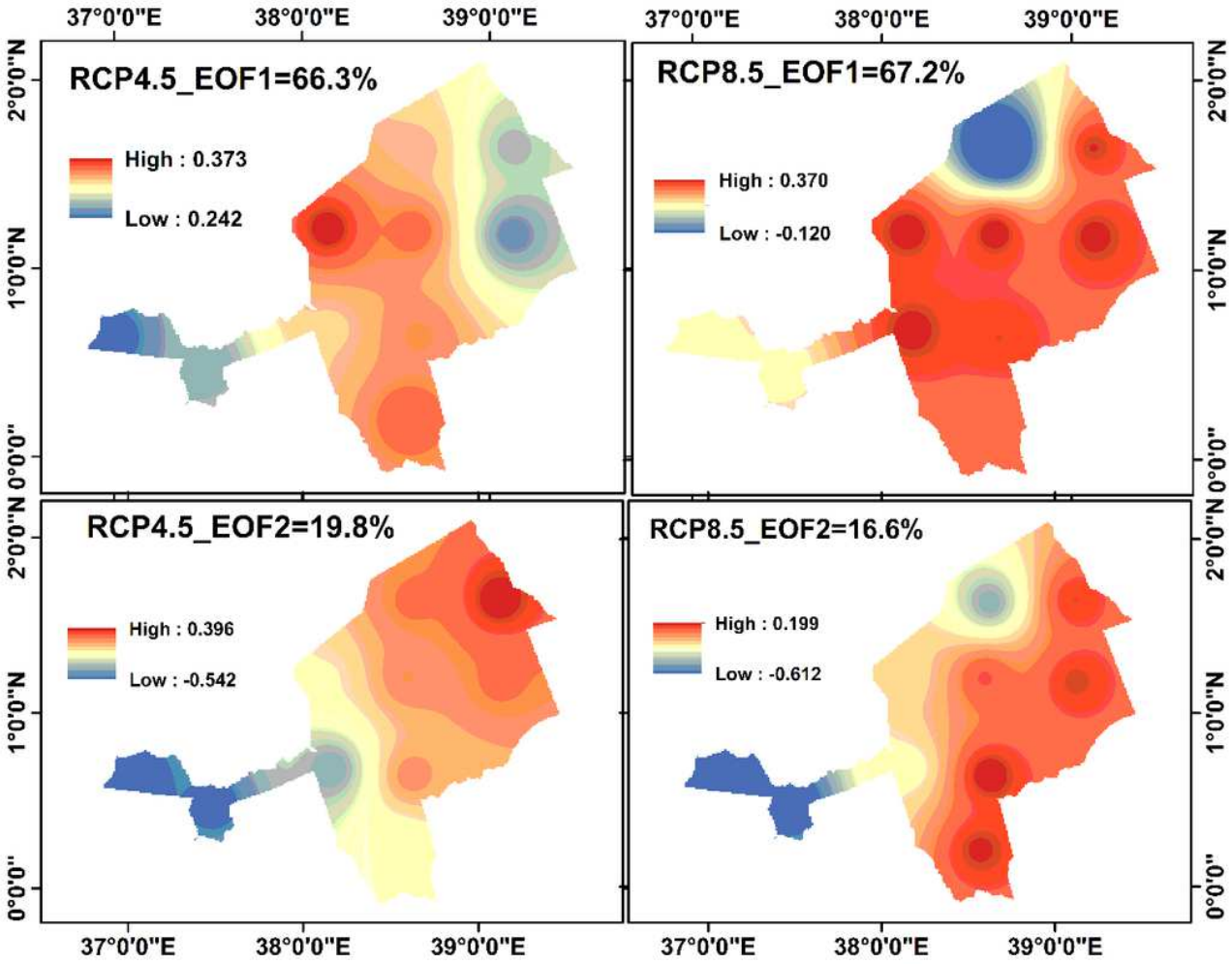

Figure 8

Spatial patterns of first two dominant EOF loadings for projected (2020-2050) scPDSI in Isiolo County, Kenya

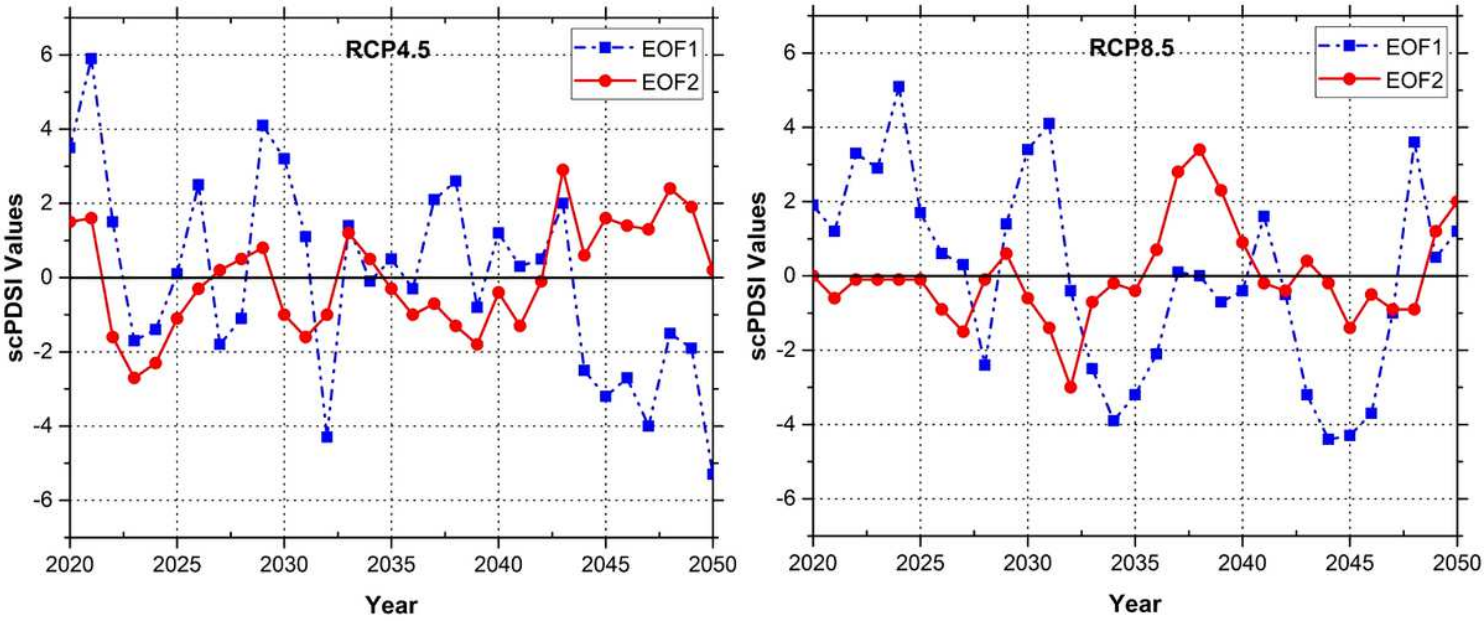

Figure 9

The temporal pattern of EOF scores corresponding to the first two dominant loading for projected (2020-2050) scPDSI

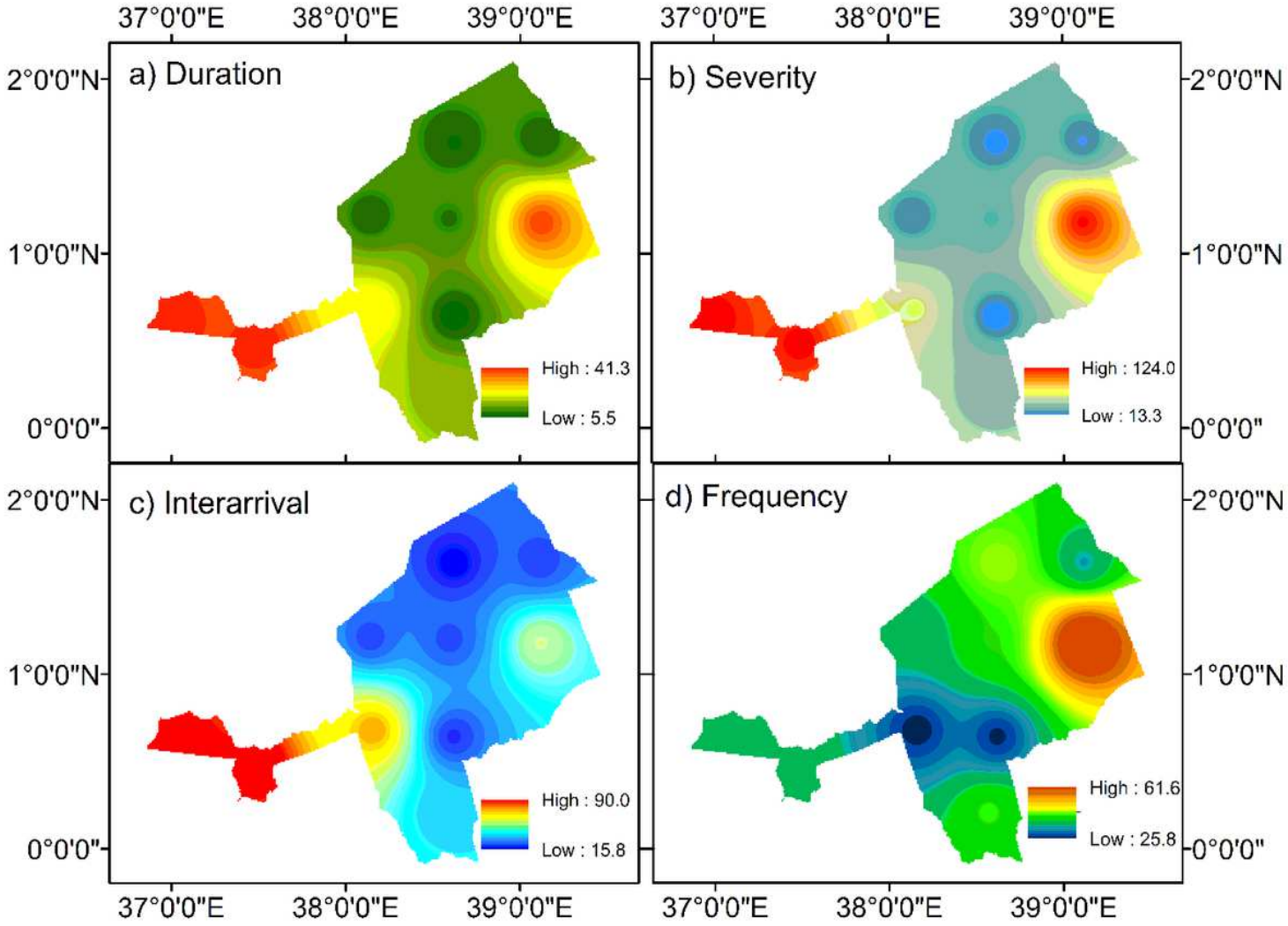

Figure 10

Projected drought characteristics under RCP4.5 (scPDSI ≤ - 1). a) Duration (Months), b) Severity c) Interarrival (Months) and d) Frequency (%)

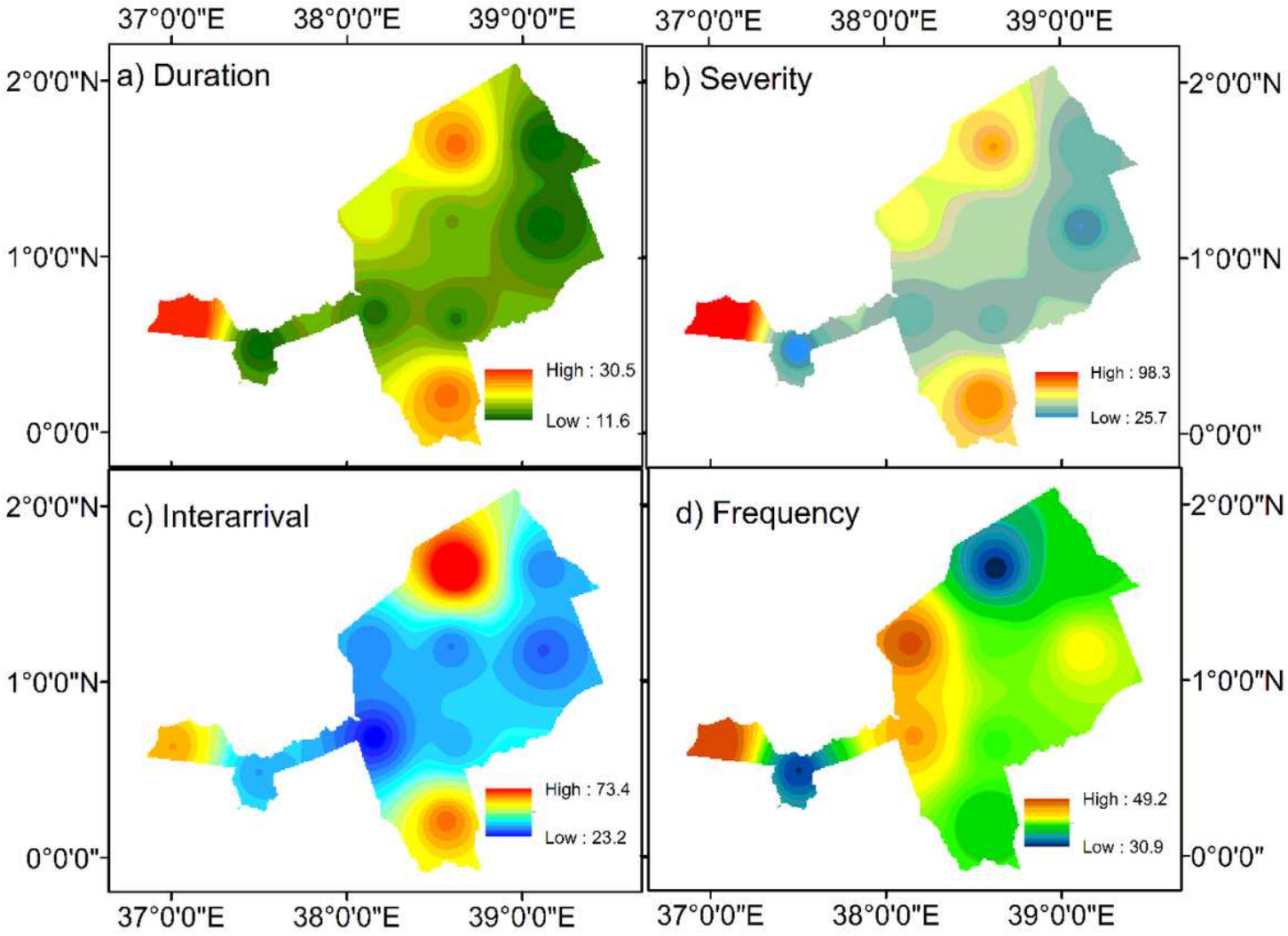

Figure 11

Projected drought characteristics under RCP8.5 (scPDSI ≤ - 1). a) Duration (Months), b) Severity c) Interarrival (Months) and d) Frequency (%)

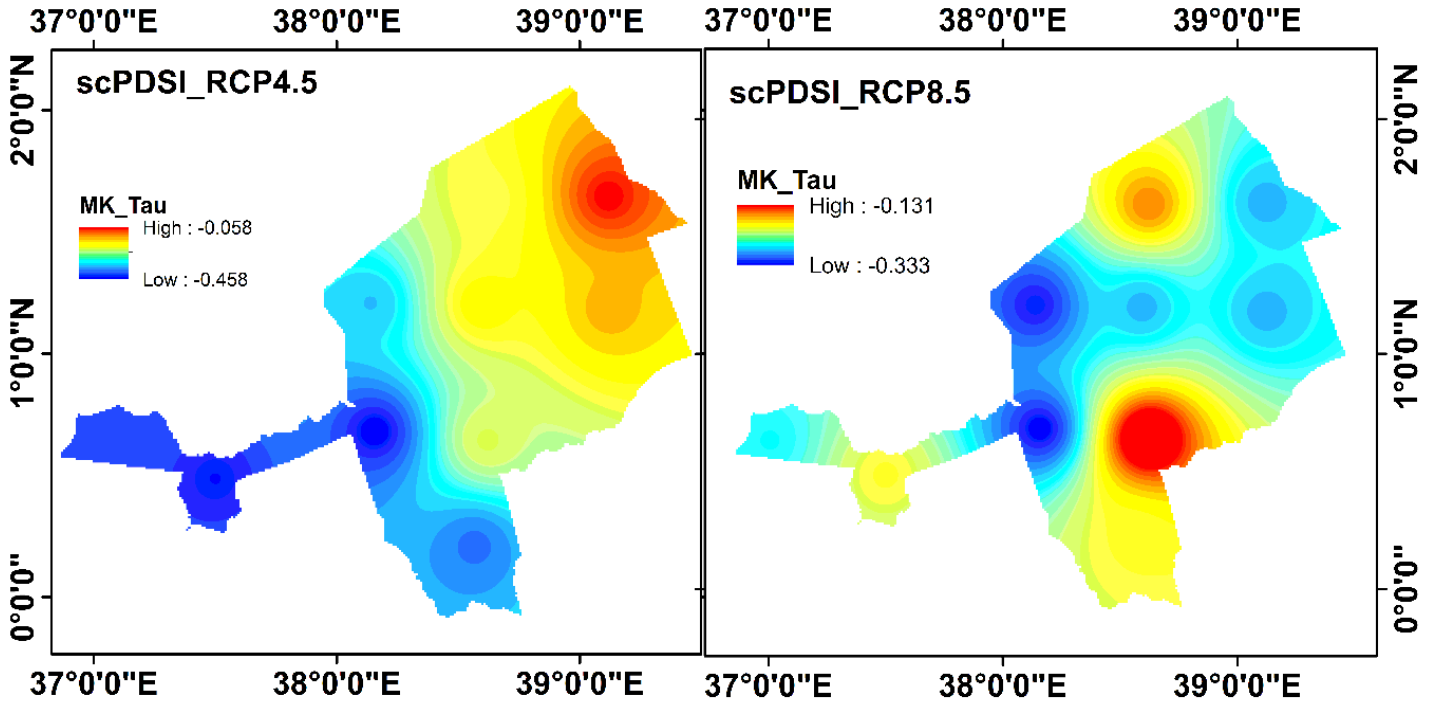

Figure 12

Spatial Mann-Kendall tau statistics of the projected (2020-2050) scPDSI RCP4.5 (left) and RCP 8.5 (right) respectively

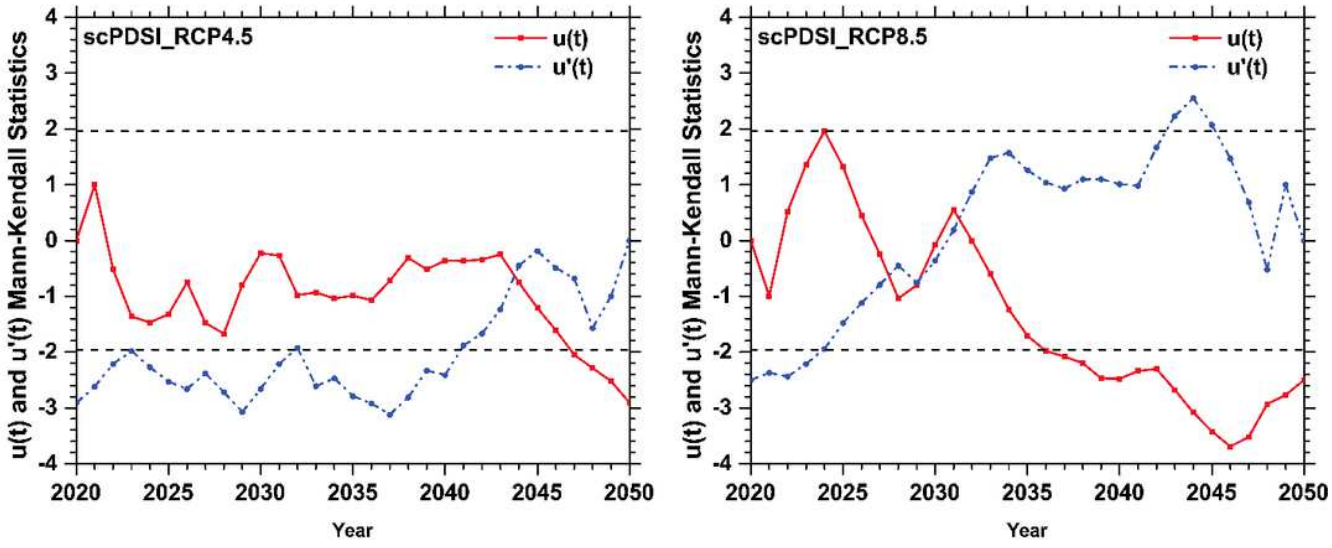

Figure 13

Sequential values of the statistics forward sequence, u(t)(solid red line) and backward sequence u' (t) (dashed blue line), the dashed black lines indicate the 95% confidence level; upper limit 1.96 and lower limit -1.96 respectively from the Mann-Kedall sequential test. scPDSI RCP4.5 (left), scPDSI RCP8.5 (Right)

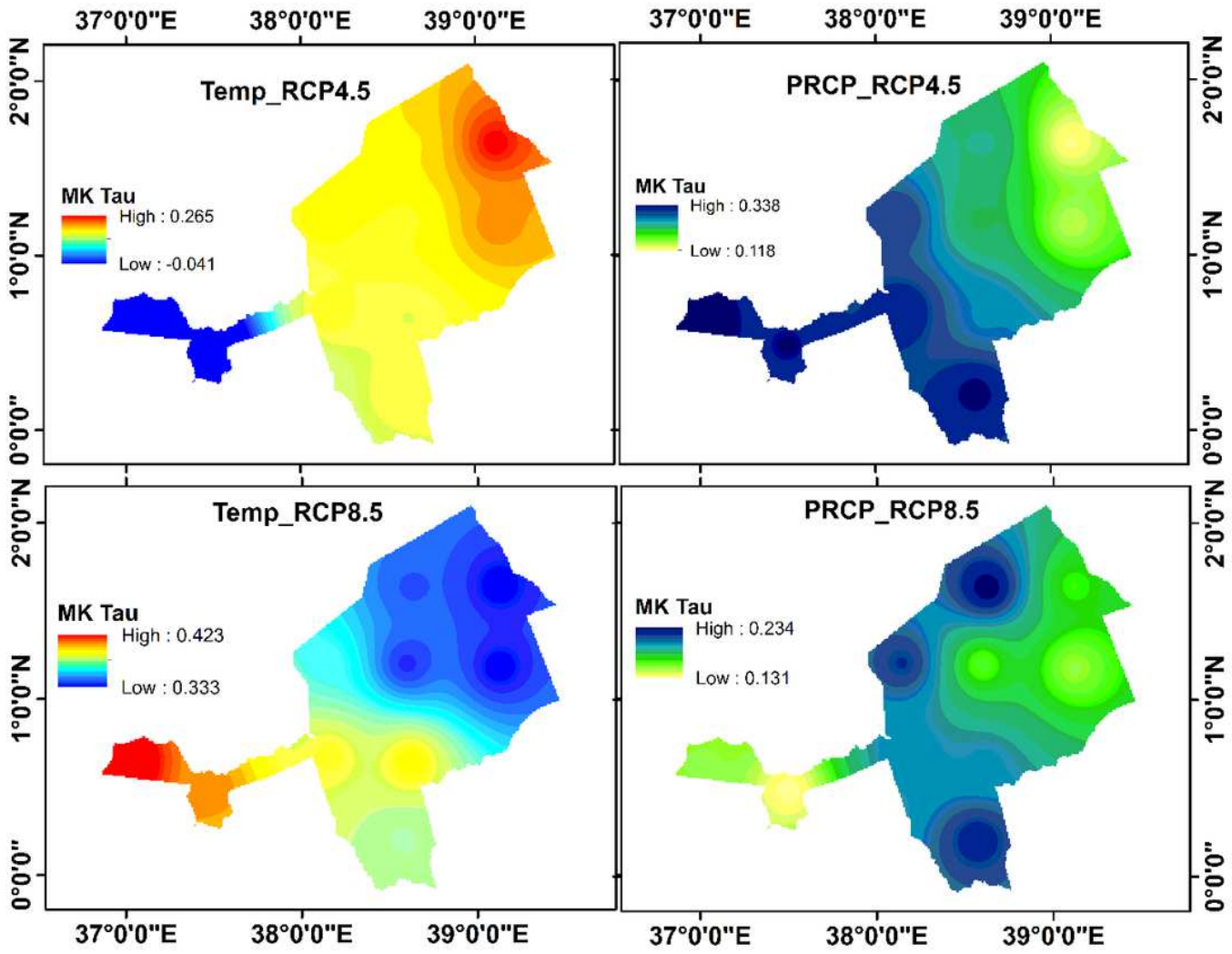

Figure 14

Spatial Mann-Kendall tau statistics of the projected (2020-2050) temperature RCP4.5 (top-left), temperature RCP 8.5 (bottom-left), rainfall RCP4.5 (top-right), rainfall RCP 8.5 (bottom-right)

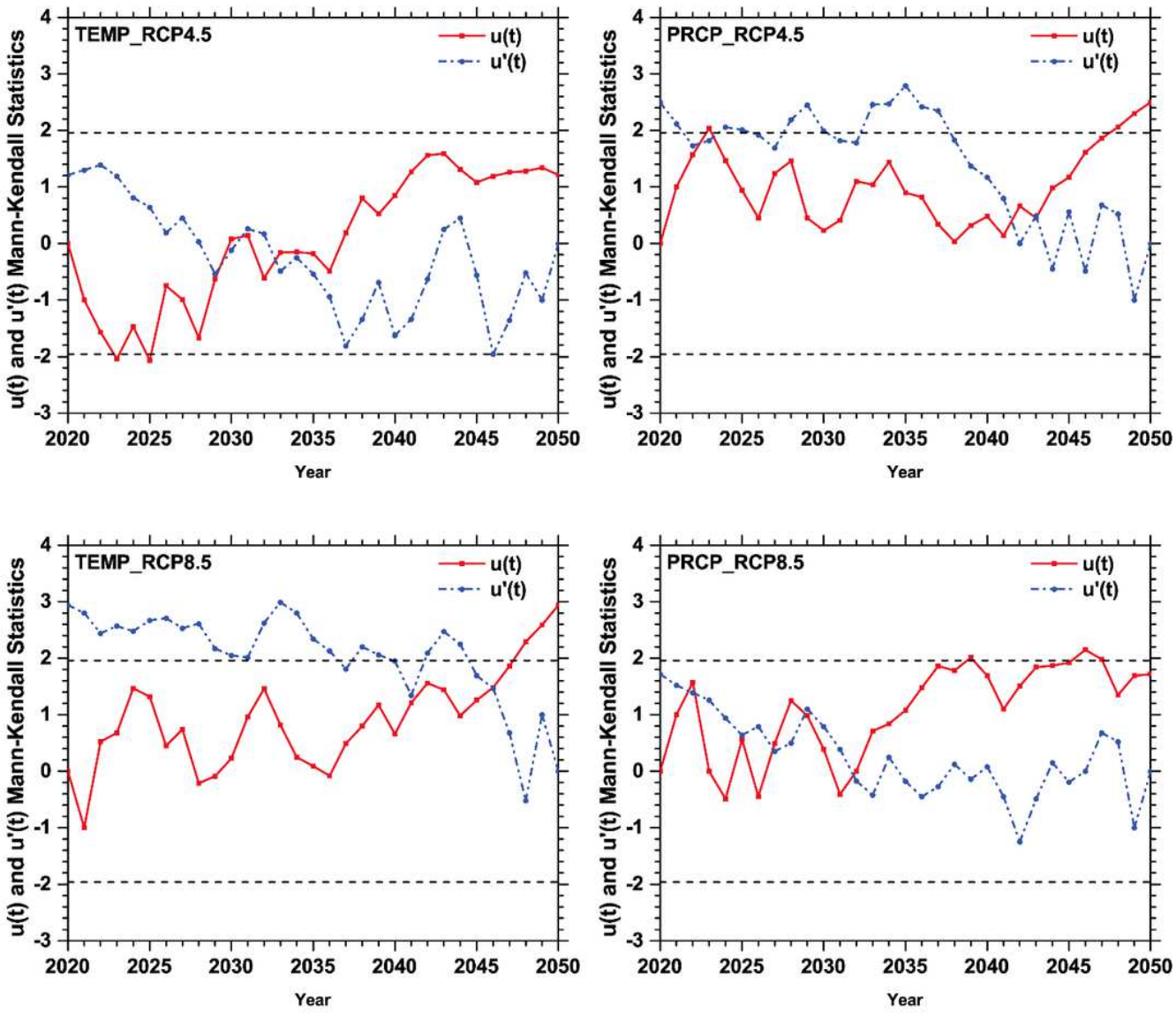

Figure 15

Sequential values of the statistics forward sequence (Fw Seq_t), u(t)(solid red line) and backward sequence u' (t) (dashed blue line), the dashed black lines indicate the 95% confidence level; upper limit (UL) 1.96 and lower limit (LL) -1.96 respectively from the Mann-Kedall sequential test. Temperature RCP4.5 (top-left), temperature RCP8.5 (bottom-left), precipitation RCP4.5 (top-right) and precipitation RCP8.5 (bottom-right)